



Introduction to Underwater Vision

Computer Vision and
Robotics Institute

Nuno Gracias, Rafael Garcia &
Ricard Campos



Schedule for today

PART 1

- Introduction to underwater Vision
- Pre-processing

PART 2

- Feature detection and description
- Feature matching

PART 3

- Motion estimation and outlier rejection

PART 4

- Topology Estimation and Global Alignment



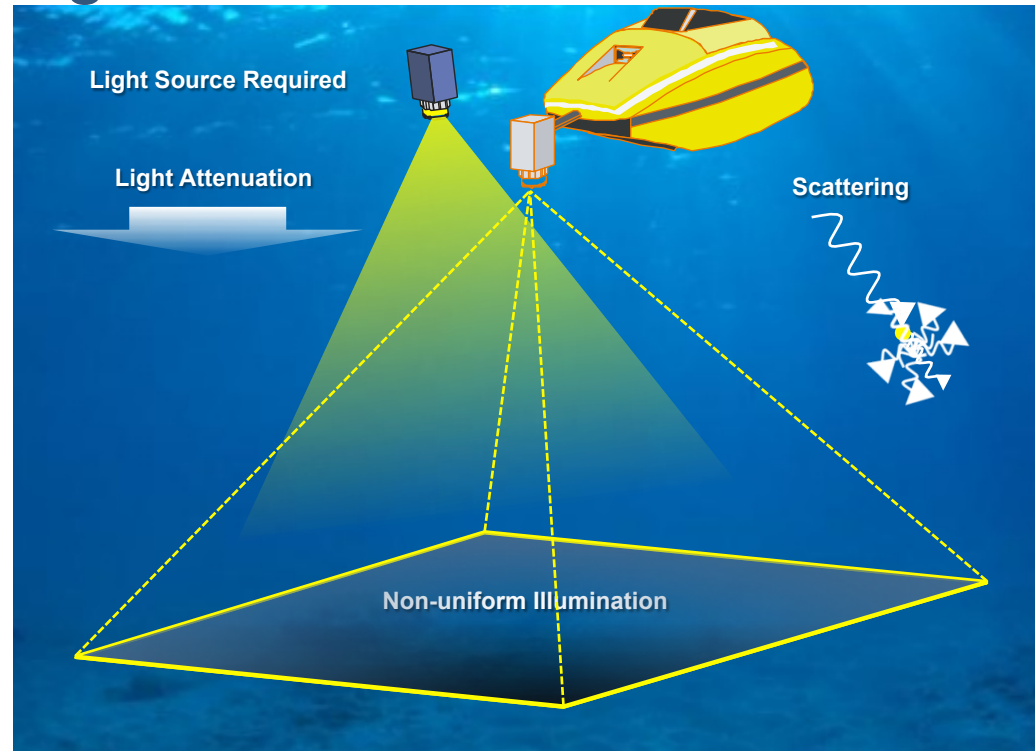
PART 1

- Introduction to underwater Vision
- Pre-processing

Using vision underwater, uhm...

❖ Light and water are not good friends:

- Absorption
- Scattering
- Blurring
- Non-uniform lighting



- ## ❖ We need to get close to the seafloor to collect data → data gathering is expensive

Underwater imaging

- Poor visibility
- Distance dependent

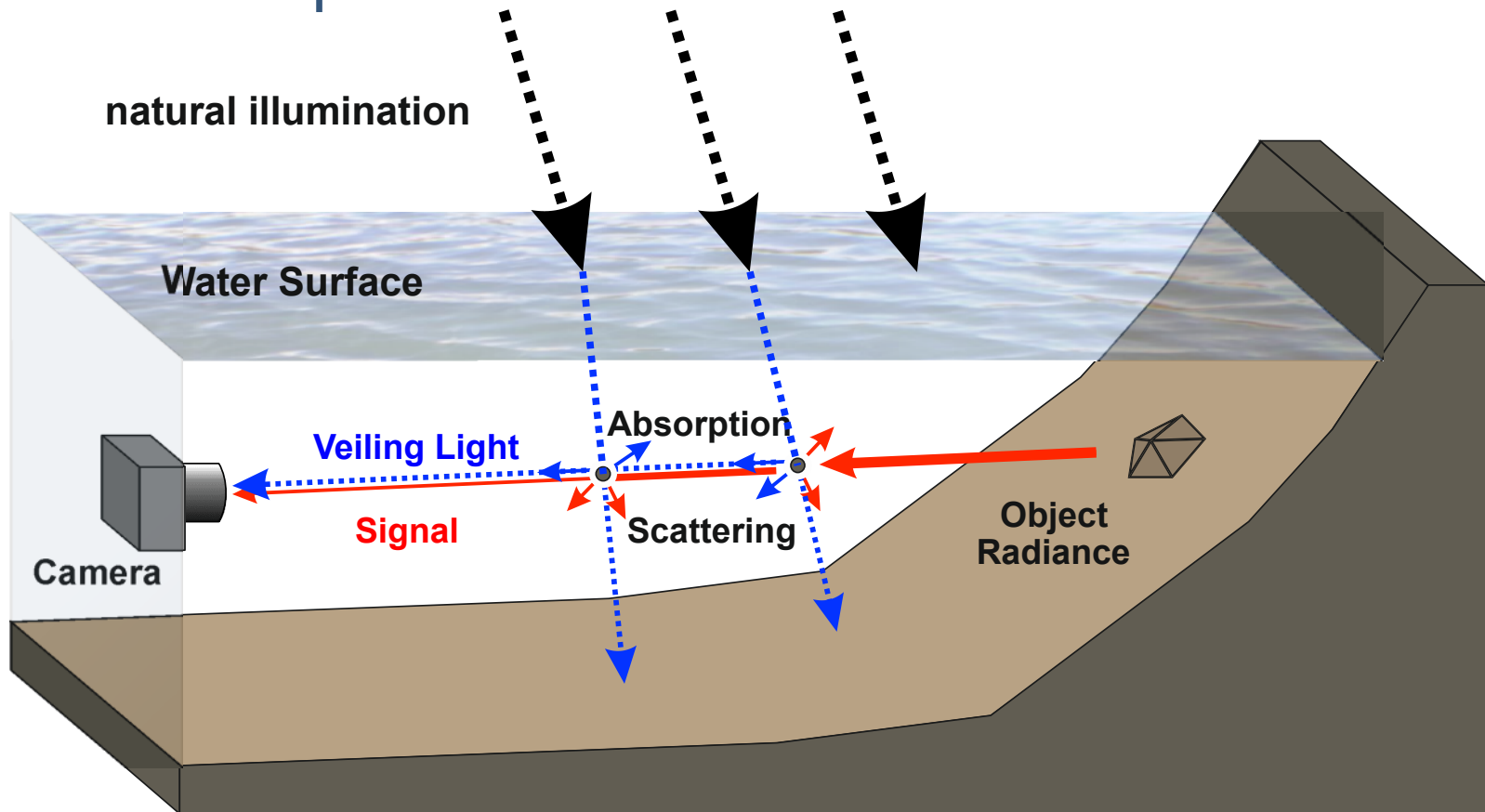


*Kahanov and Royal

Underwater imaging

Veiling light = Spacelight = Path radiance = Backscatter

- Poor visibility
- Dist. dependent

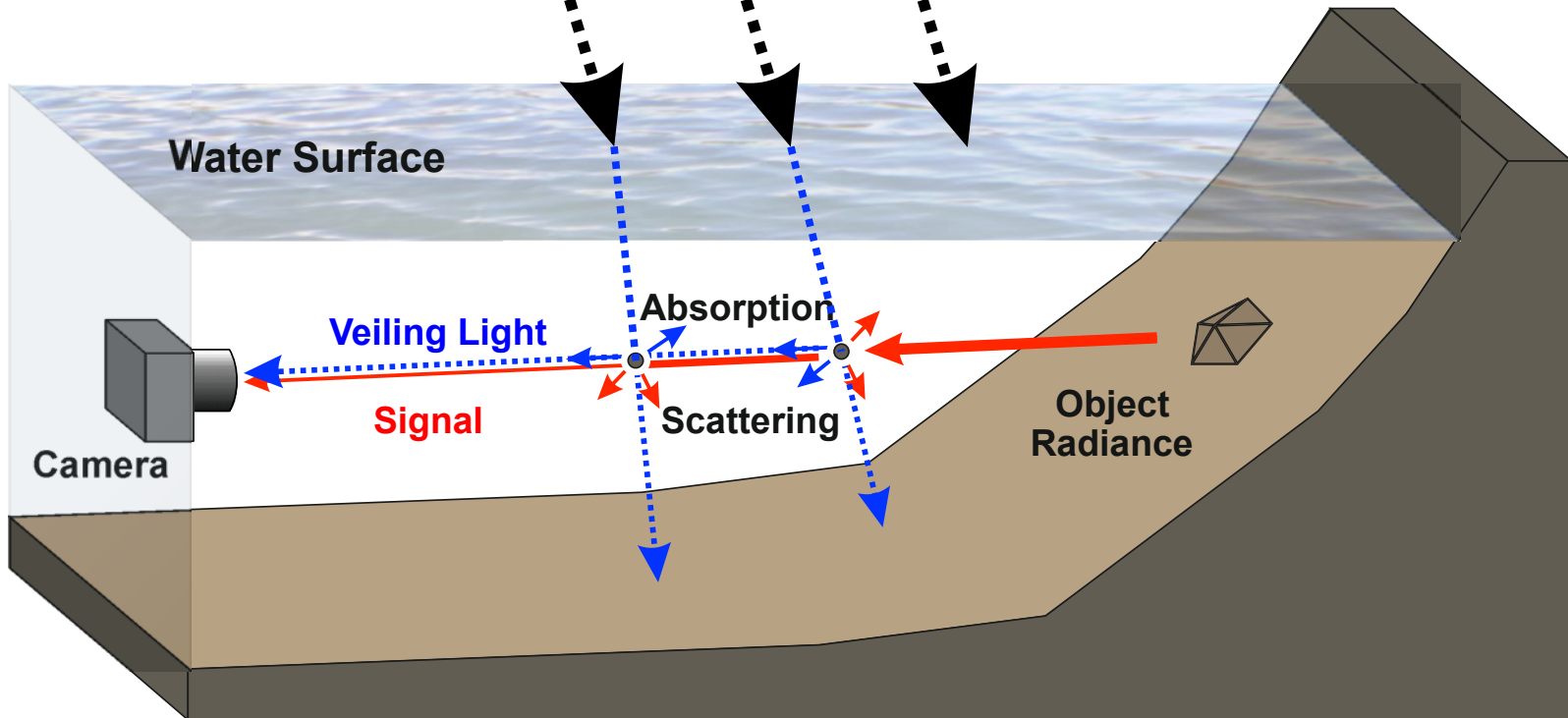


Underwater imaging

$$I(x) = J(x) \cdot t(x) + A(x) \cdot (1 - t(x))$$

Scene radiance · *transmission*; $t \in [0,1]$

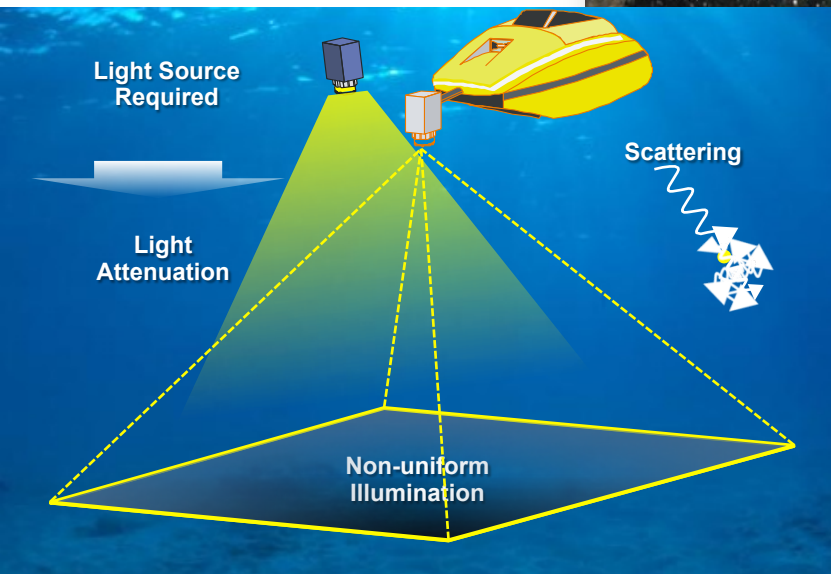
Airlight constant



Underwater imaging

❖ Scattering

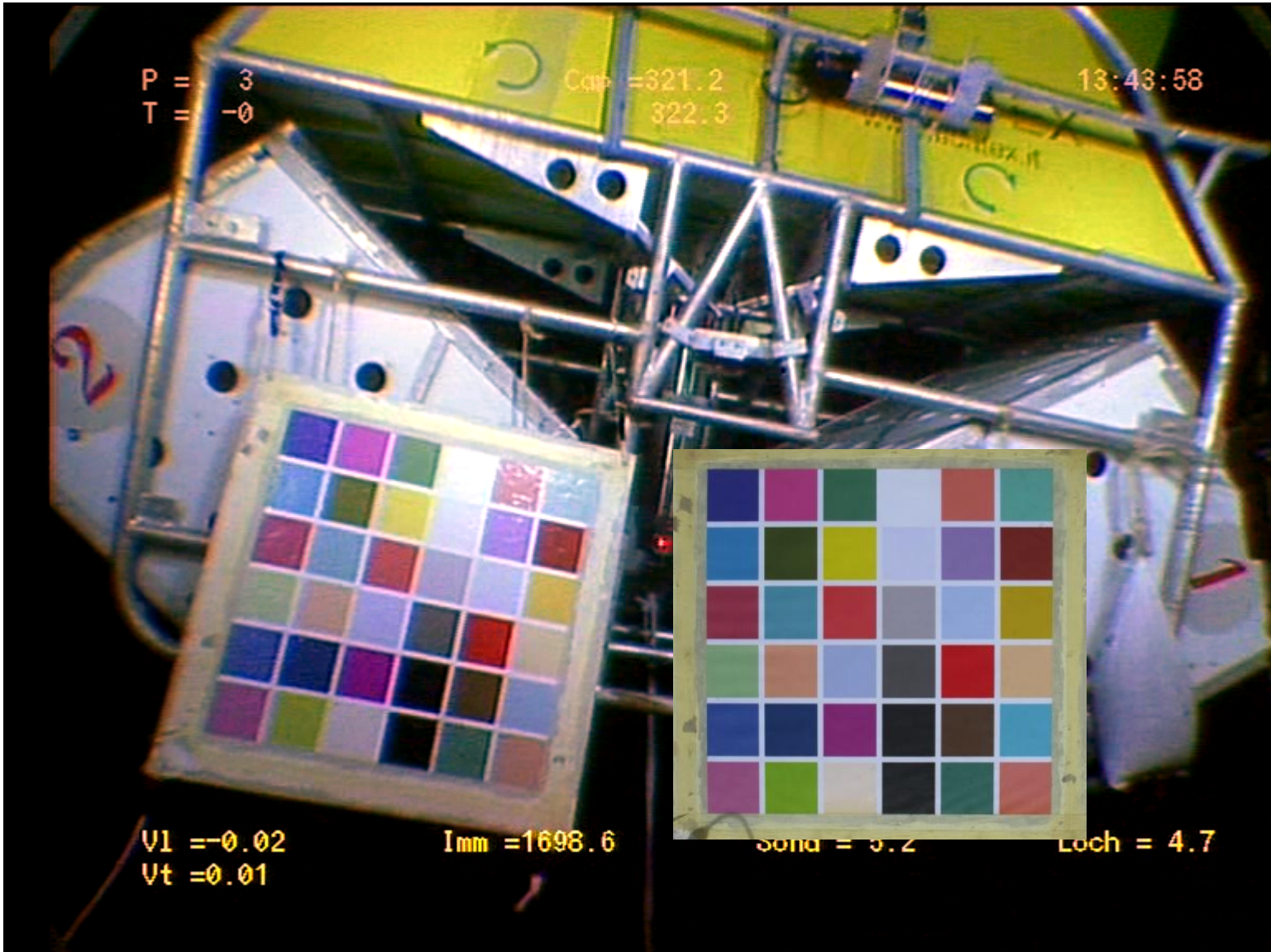
Lakeland Shipwreck – Lake Michigan, ~67m depth



(<http://www.nordicdiver.com>)

Underwater imaging

Bathyluck cruise (2009). PI: Javier Escartin



Photometric Artifacts: summary

Underwater Imaging Environment



Sun Flicker (caustics)
Cast Shadows
Suspended Particles
Turbulence

High Turbidity
Visual Cues from
Natural Features and
Manmade Structures



Artificial Lighting

Back-Scatter

Visual Cues from floating Life
Forms (marine larval ecology, e.g.,
plankton)



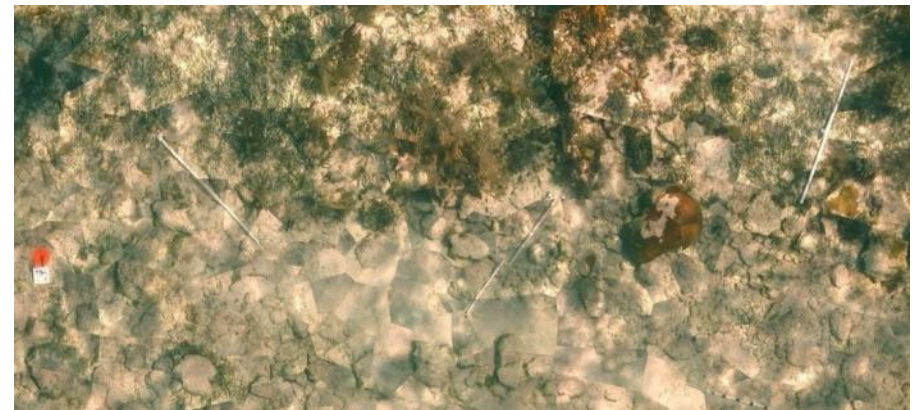
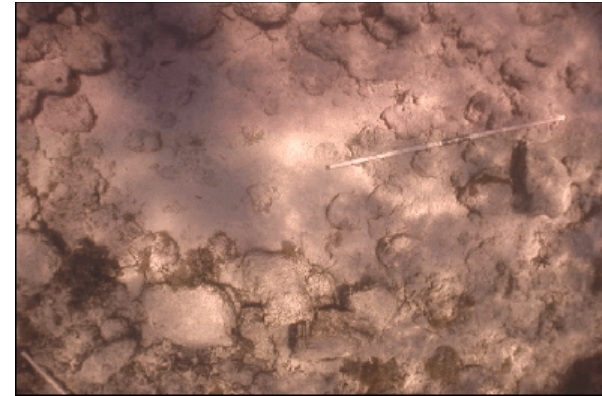
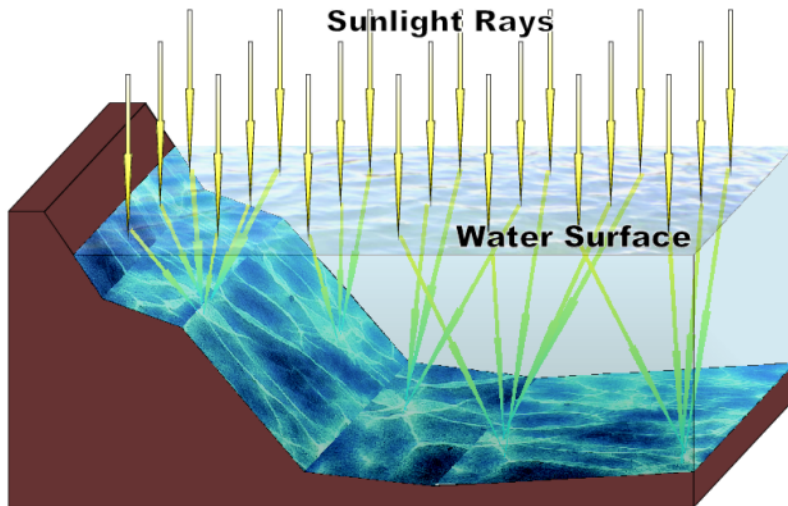
Artificial Lighting
Shading
Cast Shadows

Loss of Color
Strong Visual Cues
from Benthic
Features



Removing sunlight flicker

Refracted sunlight creates irradiance (light) fluctuations



Refracted Sunlight

- Can disrupt image processing algorithms (matching and segmentation)
- Makes it harder to interpret benthic structures

Our Approach – 2 key observations

❖ *Observation 1*

- The difference between an image and the temporal median *has two components*

Component 1 – Instant illumination field from sun light

Component 2 – Artifacts from registration errors

Original image



Temporal Median



Difference



Our Approach – 2 key observations

❖ *Observation 2*

- The two components are (usually) *easily separable in the frequency domain*

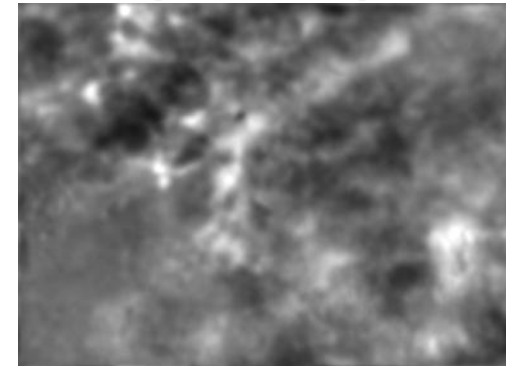
Difference



**Low Pass
Filter**



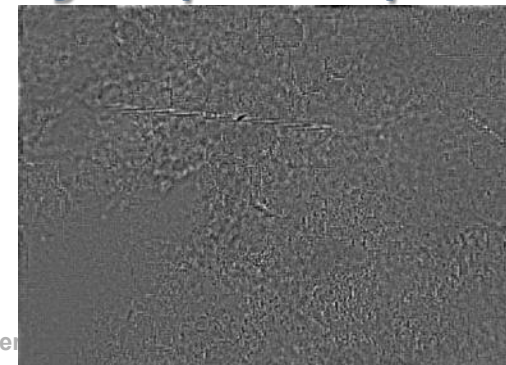
***Illumination field has
lower spatial frequencies***



**High Pass
Filter**



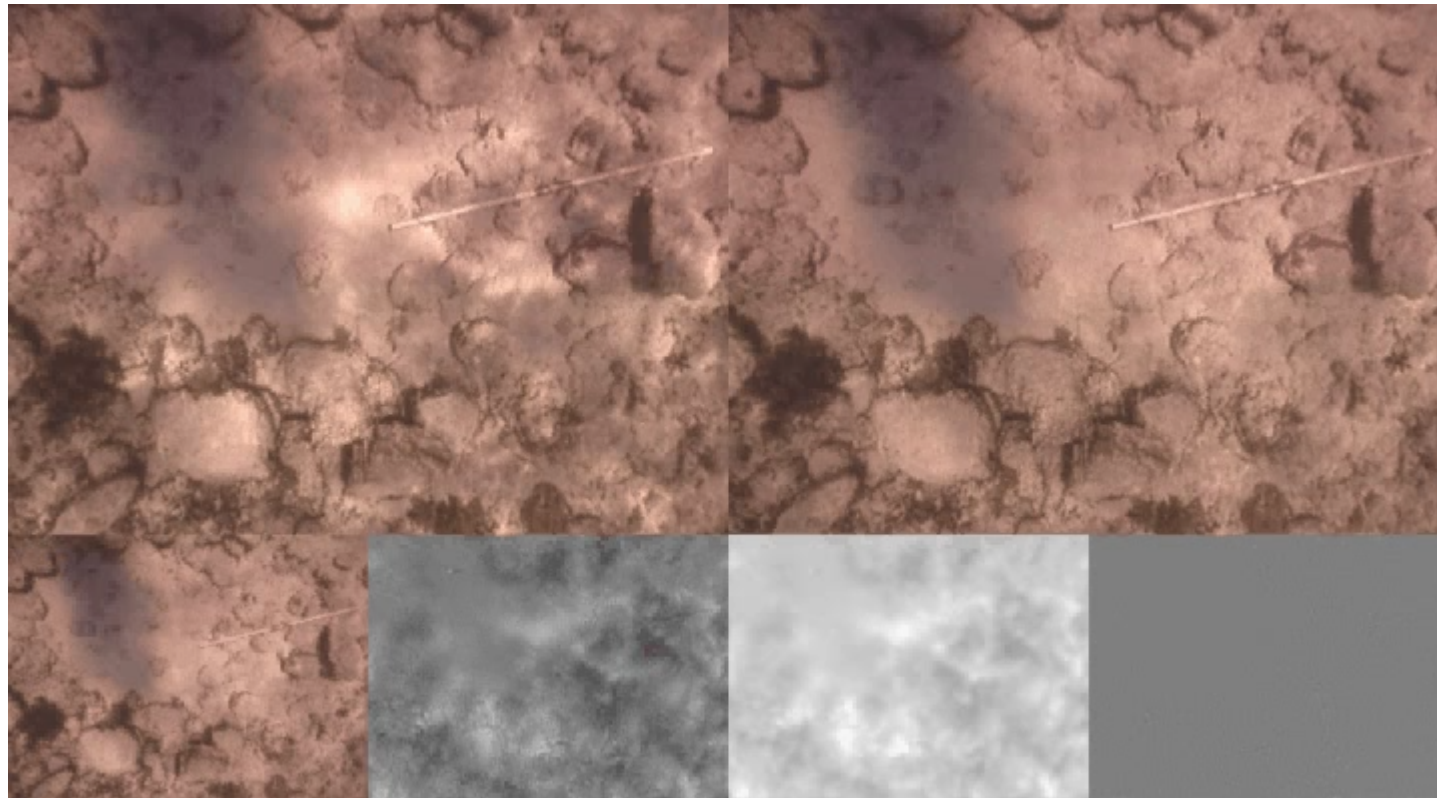
***Registration artifacts have
higher spatial frequencies***



Removing sunlight flicker

Input

Output



Temporal Median

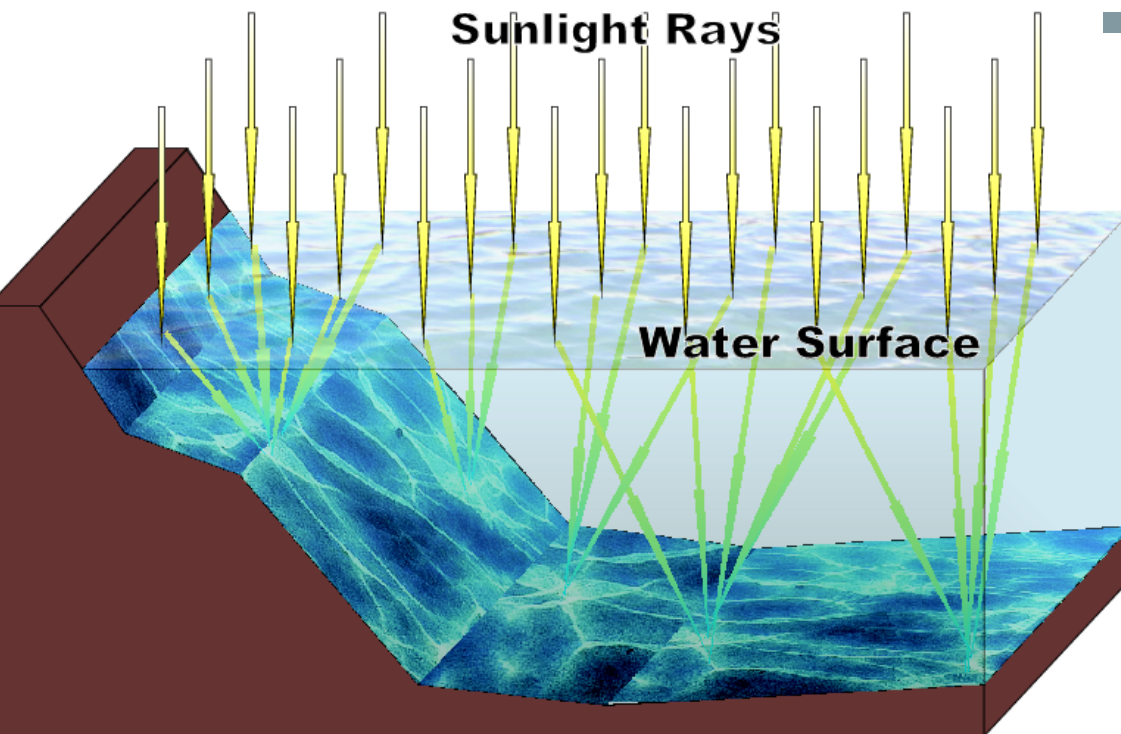
Difference
(Input - Median)

Illumination field
(low pass difference)

Residue
(Output - Median)

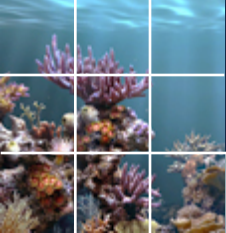
sunlight flicker revisited

- Created by refracted sunlight
- Degrades image quality and the information content
- Inversely proportional to depth

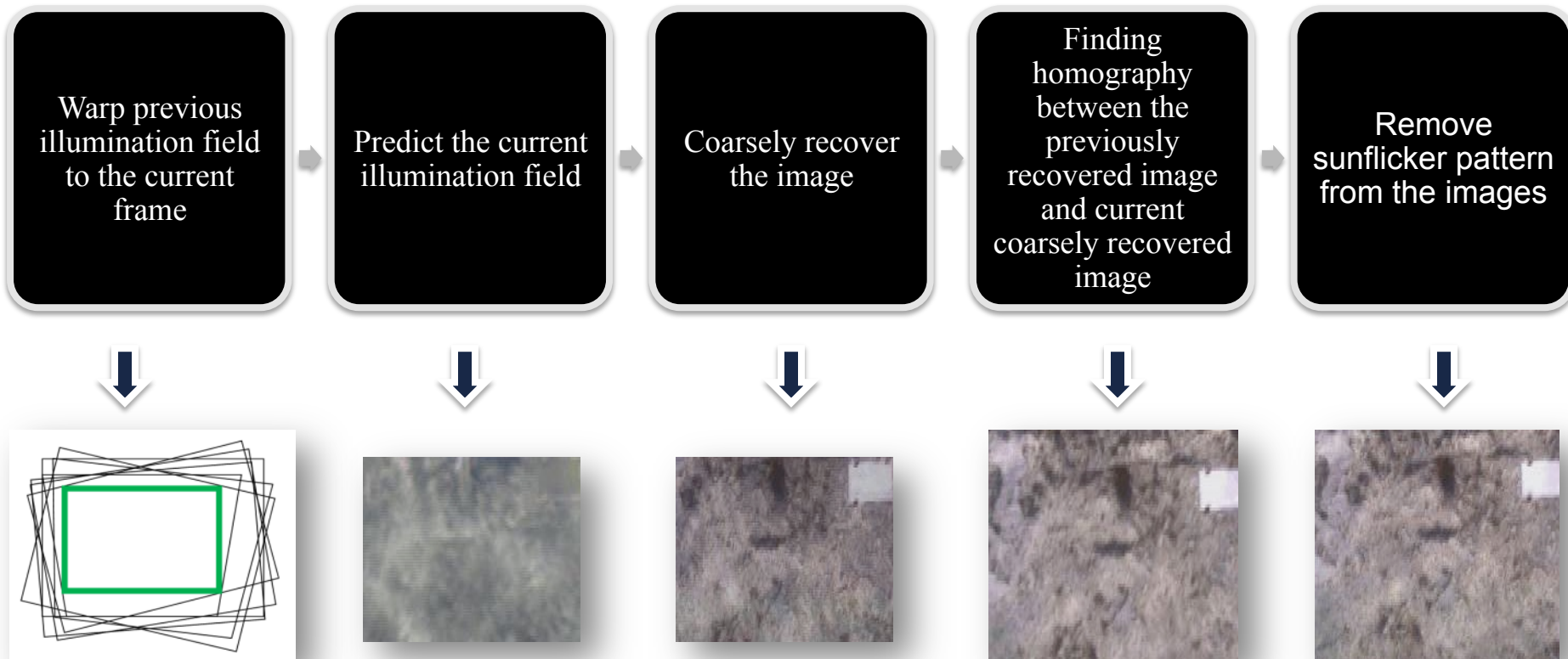


- **Generates dynamic patterns**

Wu Y. N. Doretto G., Chiuso and S. Soatto. Dynamic textures. Journal of Computer Vision, 2003, Kluwer Academic Publishers, pages 51(2): 91-109, 2003.



Pipeline



Assumptions:

1. Illumination field is a dynamic texture
2. Smooth camera movement
3. Flat (approximately) bottom of the sea

Dynamic texture modeling



1



2



3



1. Input image
2. Coarsely recovered image
3. Finally recovered image
4. Original illumination field
5. Predicted illumination field
6. Median image

4

5

6

A. Shihavuddin, N. Gracias, R. Garcia. "Online Sunflicker Removal using Dynamic Texture Prediction".
International Conference on Computer Vision Theory and Applications, pp. 161-167, Rome (Italy).



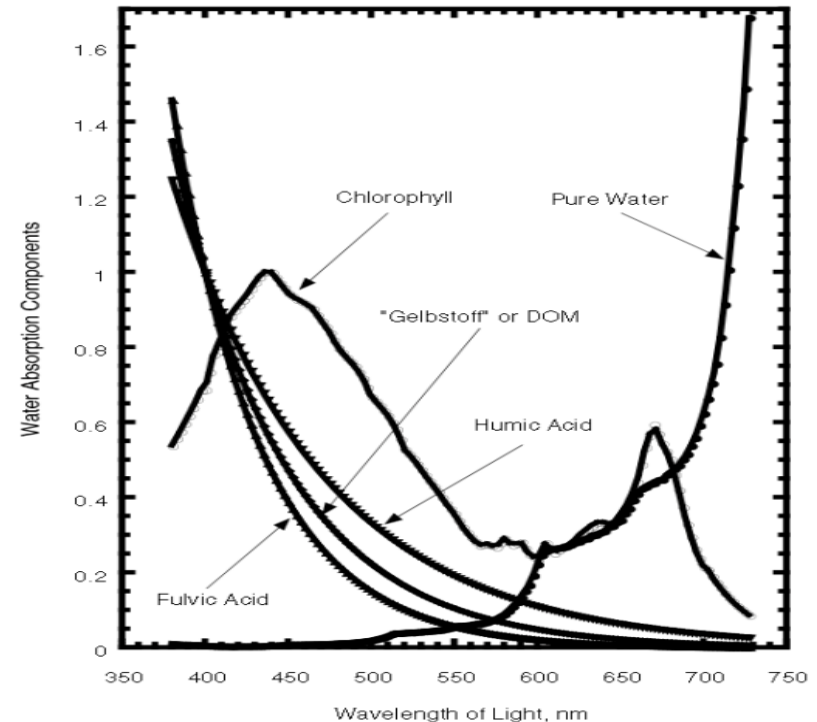
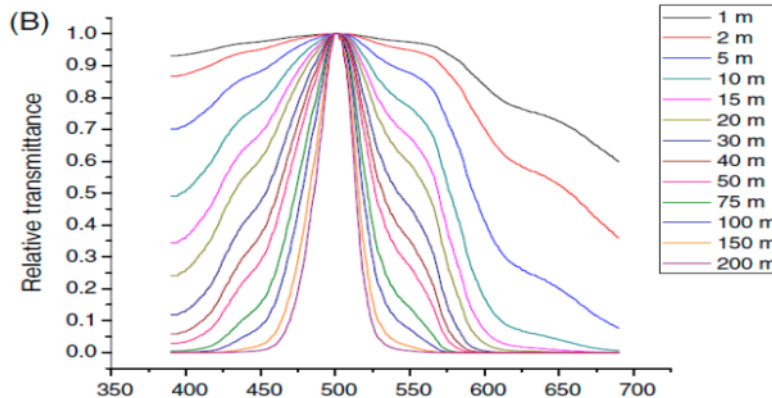
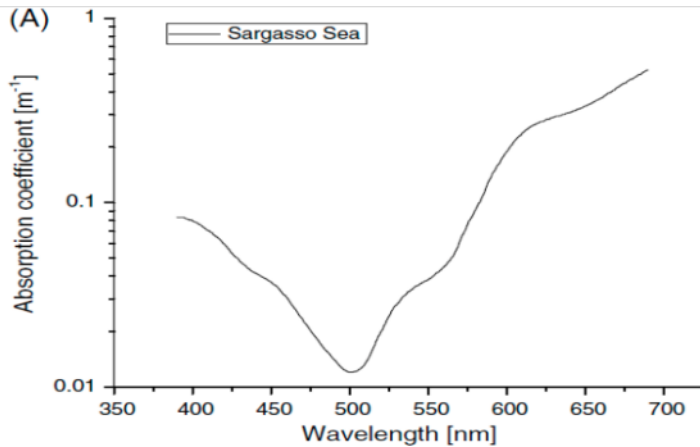
Light effects in Underwater Imaging

- ❖ **Poor visibility: light interactions with water molecules and impurities dissolved and suspended in water**
 - **Absorption effects**
 - **Scattering effects**
 - Forward scattering
 - Backward scattering
 - Fluorescences of biological objects
 - Swimming macroscopical particles
 - Lighting inhomogeneities
 - Shallow water: sun flickering
 - Deep water: artificial lighting, vignetting, limited lightpower

Light effects in Underwater Imaging

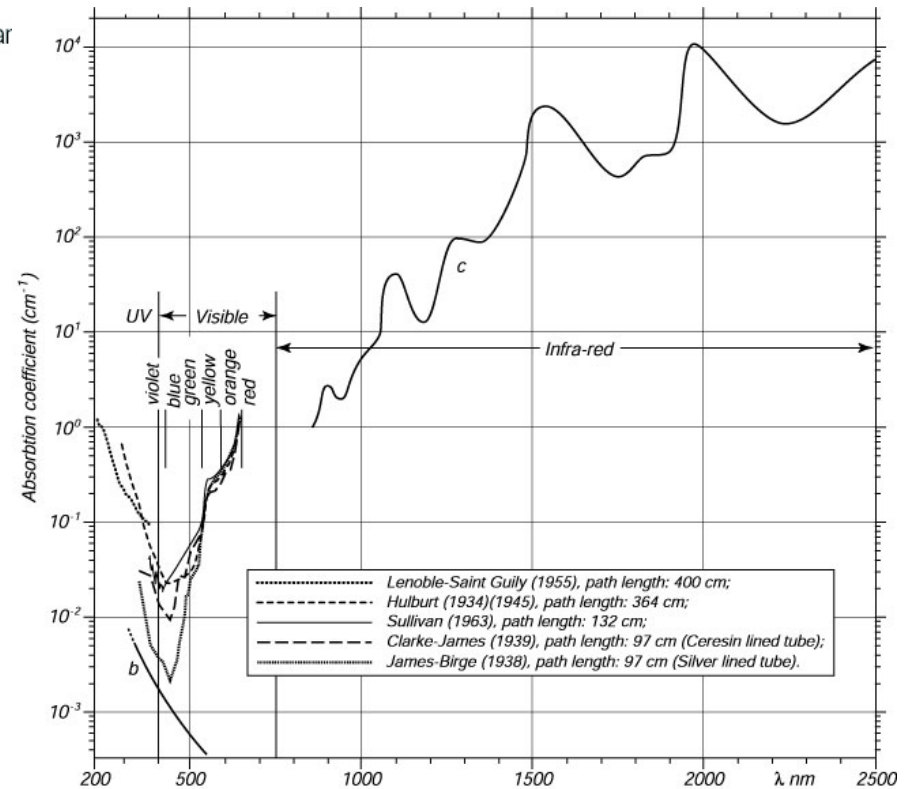
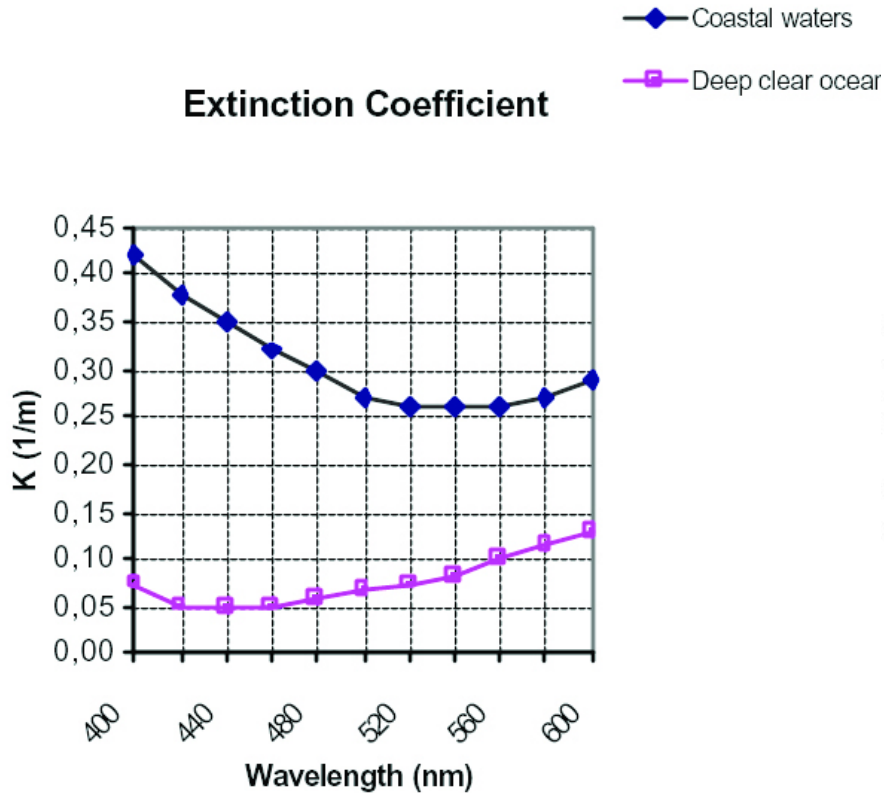
The absorption of light power is exponential - **Lambert Law of Absorption**. Attenuation Factor dependence on distance:

$F = \exp(-a(\lambda) * d)$, where $a(\lambda)$ is the spectral absorbance.

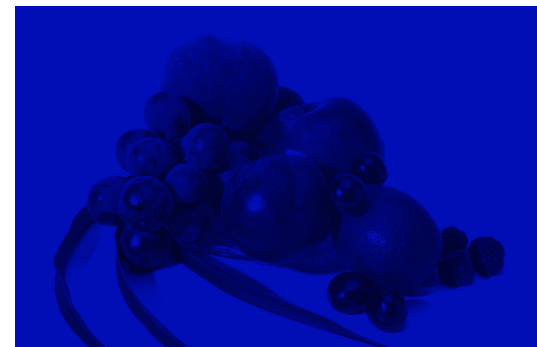
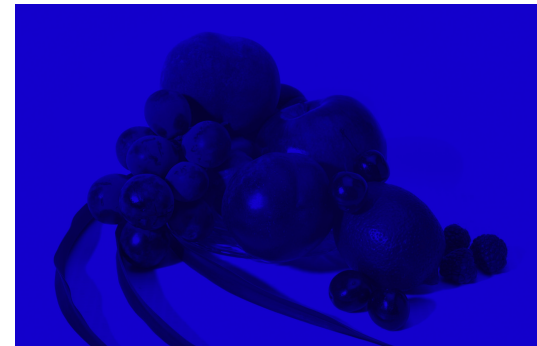
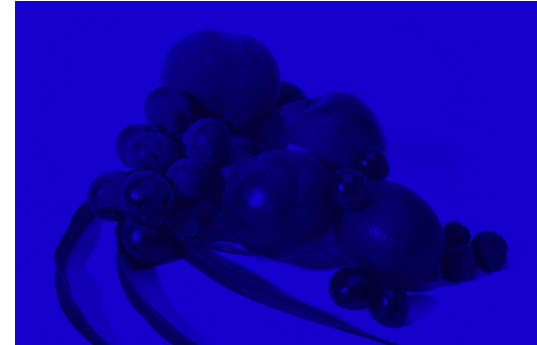
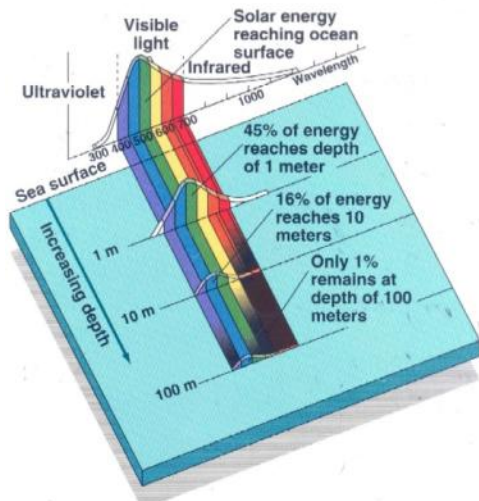
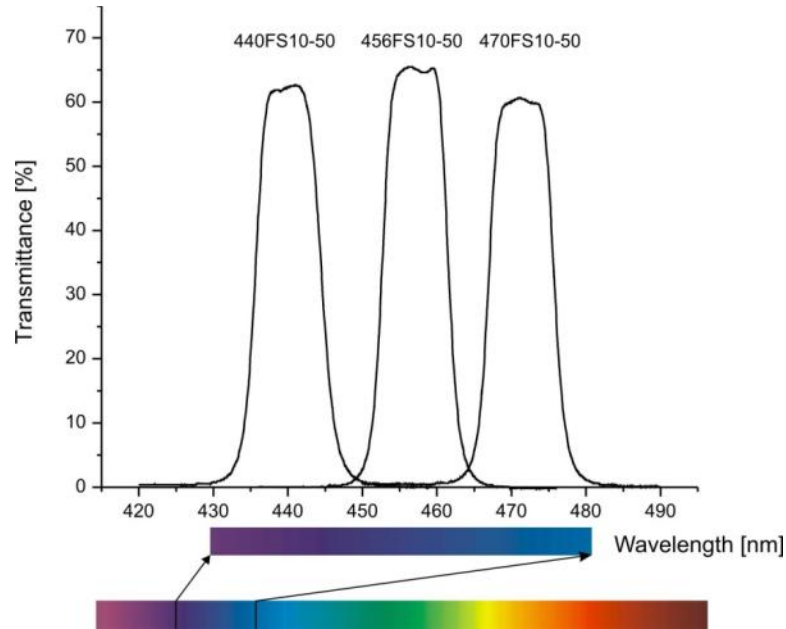


Light effects in Underwater Imaging

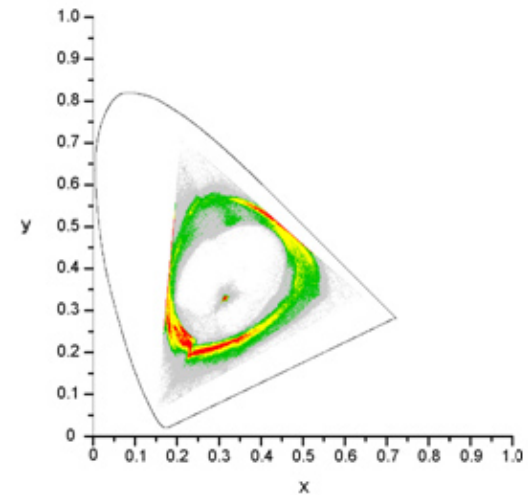
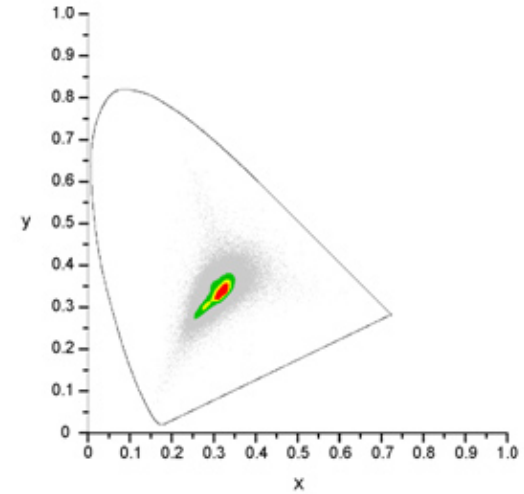
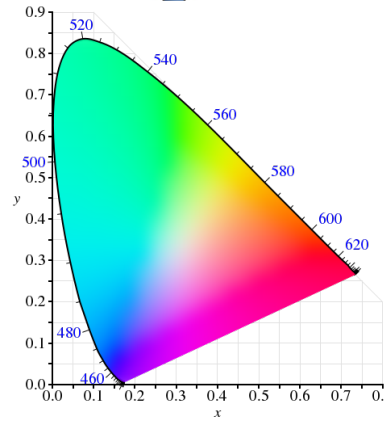
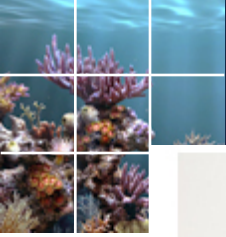
Basically, the water only is only transparent for the bluish visible range, but this range has often strong scattering effects, thereby it is loss in sharpness and contrast



A non-dehazing approach for visualization in tight blue spectral range

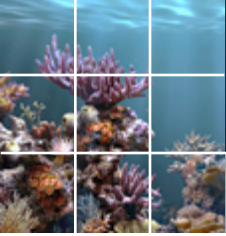


Narrow Spectral Imaging



L. Neumann, R. Garcia, J. Basa, R. Hegedus. "Acquisition and Visualization Techniques for Narrow Spectral Color Imaging", Journal of the Optical Society of America A. Vol. 30, no. 6, pp. 1039–1052, 2013.

Narrow Spectral Imaging



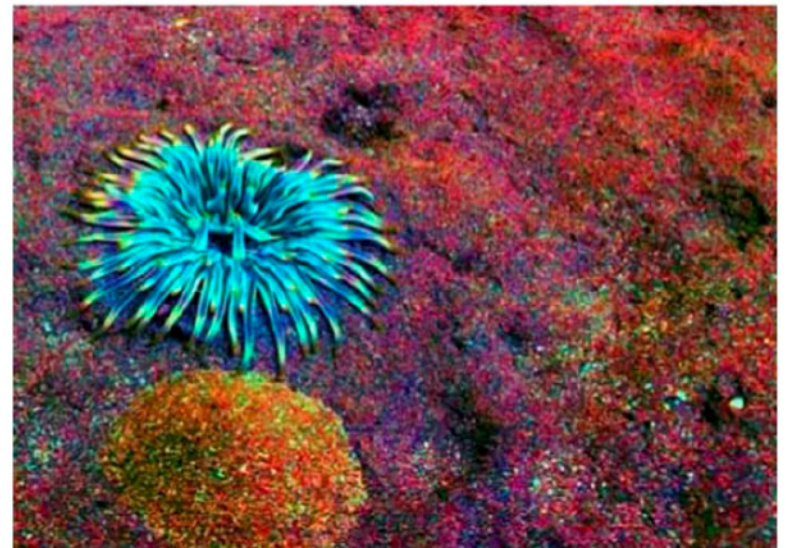
4181R W8E

Dr. Smith
12/18/08

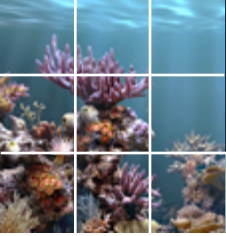


4181R W8E

Dr. Smith
12/18/08

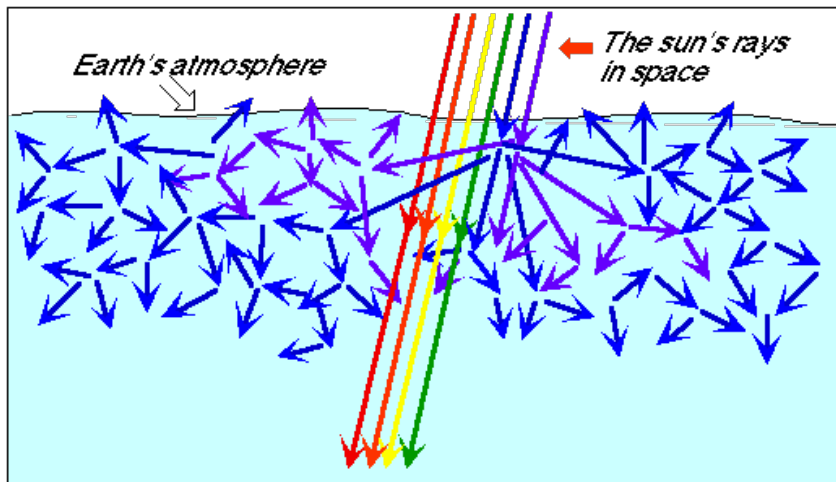


Light effects in Underwater Imaging



Rayleigh scattering results in hazy images and Mie scattering in blurry, murky, faded appearance

Density fluctuation of water molecules vs. any kind of physical inhomogeneity that is larger than water molecule (R vs. M)



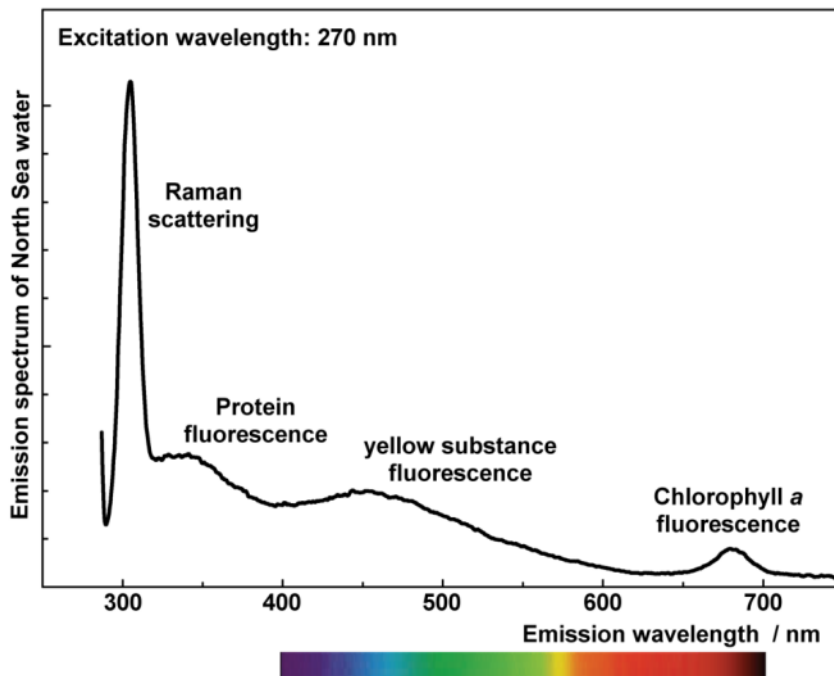
- ❖ Rayleigh angular scattering in pure water
- ❖ Appr. Wavelength's power = 4

$$\beta_W(\lambda, \vartheta) = b_W(\lambda) p_W(\cos \vartheta),$$

$$b_W(\lambda) = (0.001\,458\,4\,\text{m}^{-1}) \left(\frac{550}{\lambda} \right)^{4.34}$$

Light effects in Underwater Imaging

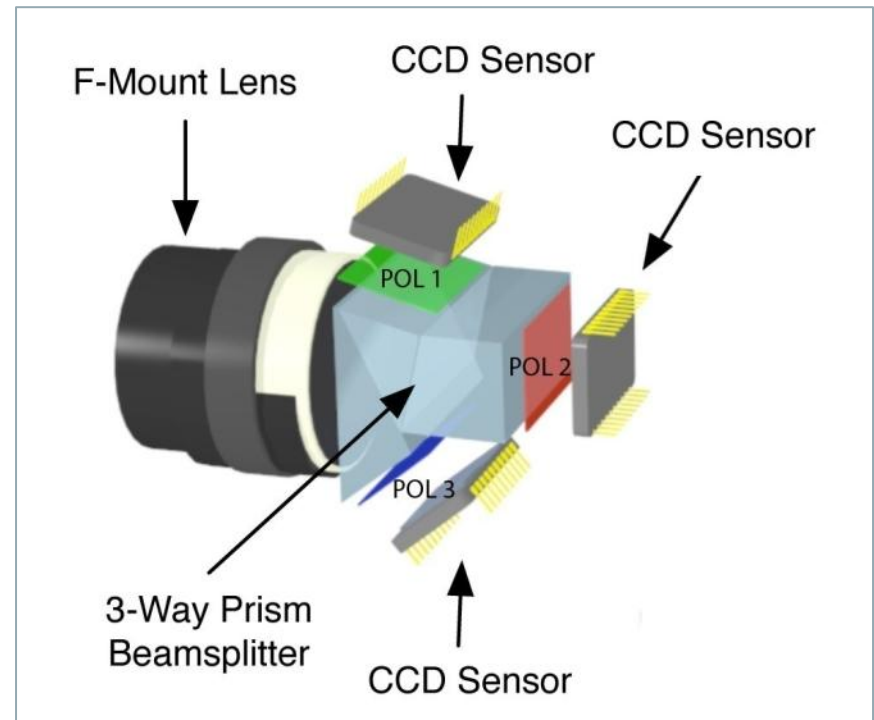
There are also natural (self illuminating) and excited fluorescence effects, characterizing some biological activities



- ❖ Fluorescence is not disturbing, low-light
- ❖ Nice and useful future work, but we do not deal with this phenomena in the **image enhancement algorithms**

Polarization

- ❖ A given part of the scattered light is linearly polarized. Polarization information can therefore be used to reduce the effect of scattered light.
- ❖ A polarization camera can acquire the full polarization information per pixel



Fluxdata Polarization camera: 3 CCD sensors with differently oriented linear polarizers



A non-underwater example with over-depolarization





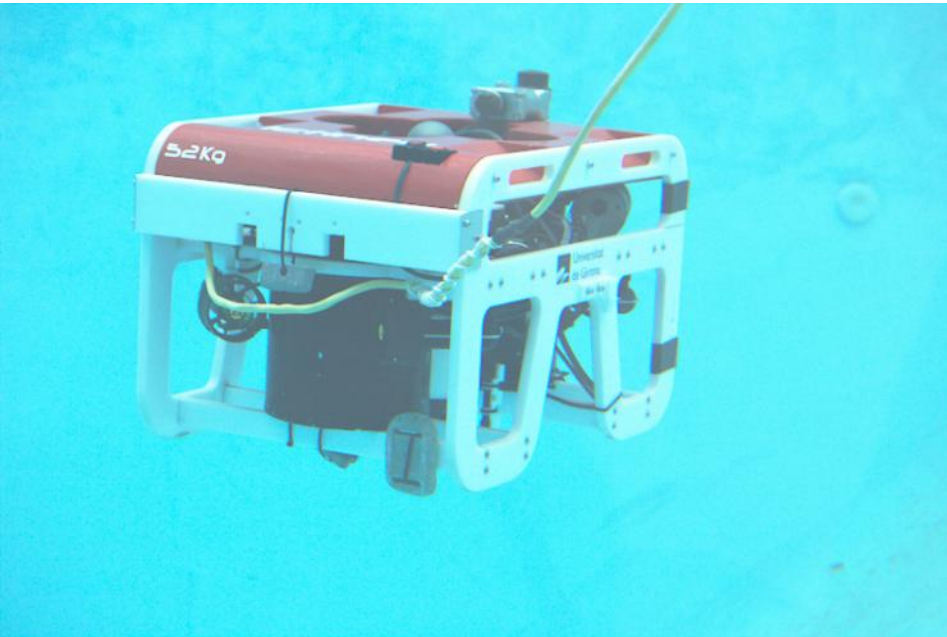
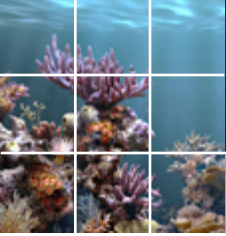
A non-underwater example with over-depolarization





Underwater dehazing examples

Underwater dehazing



Underwater dehazing

Some RED deficite, yet – in 2010 test



Underwater dehazing

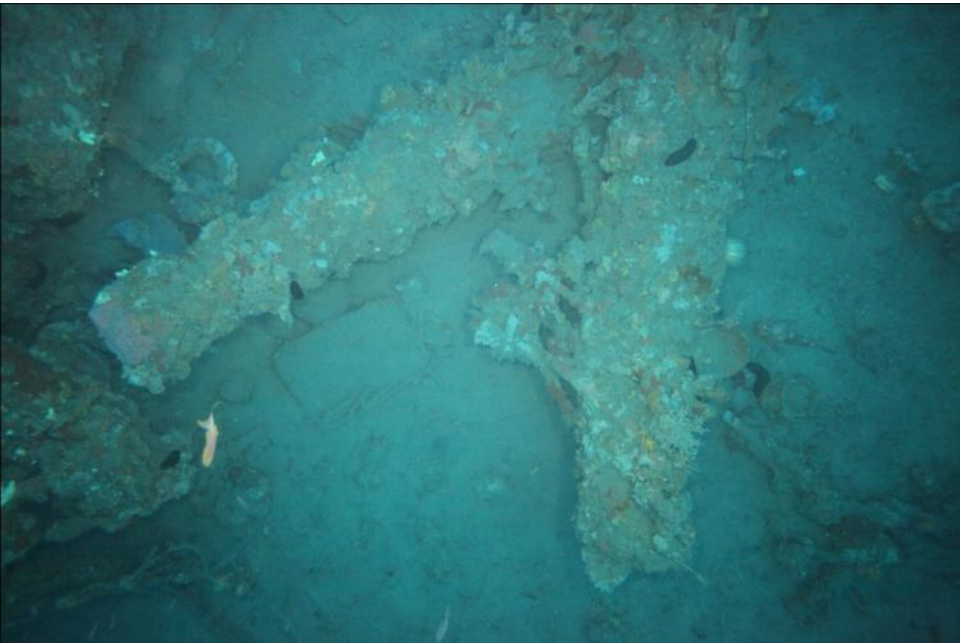


Original image



Enhanced image

Underwater dehazing



Original image



Enhanced image



Image Dehazing – Depth map approach

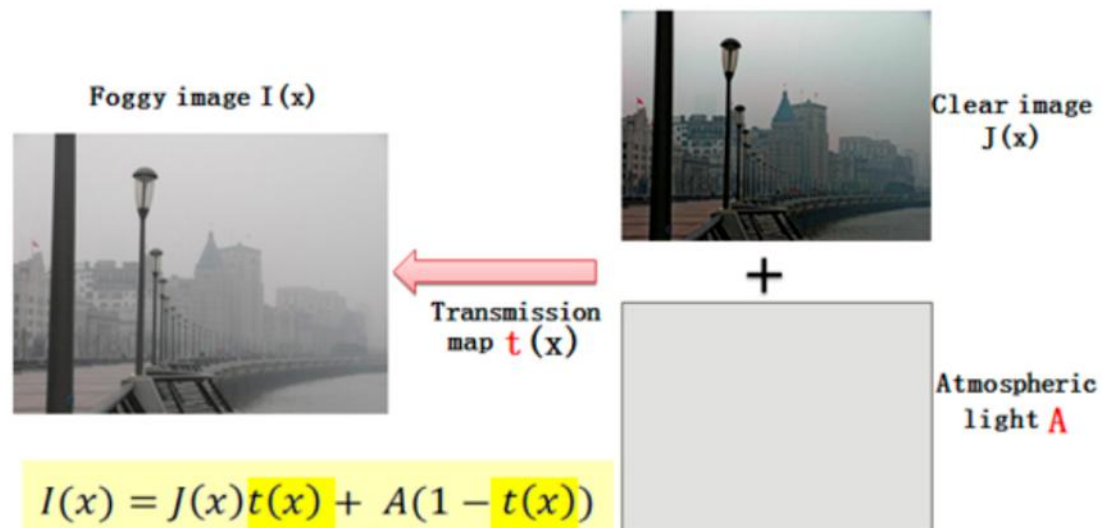
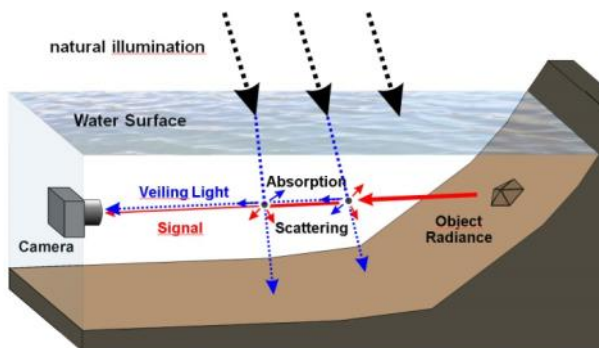
❖ Dark-channel based approach

- Based on the observation that most local patches in haze-free outdoor images contain some parts which have very low intensities in some **dark pixels** in at least one color channel, so that these will contain **only scattered** component in a hazy image

Dark Channel based Image Dehazing

❖ Basic idea

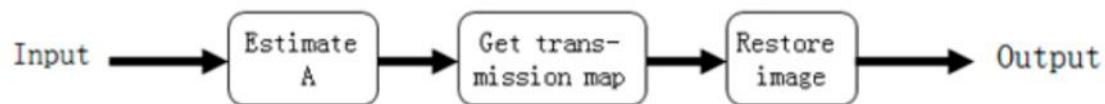
The basic idea of defogging is, foggy image = clear image + fog density. That means foggy images are clear images polluted by fog. If we estimate the fog density and remove it, then the clear image can be got. The foggy image model is shown as follows.



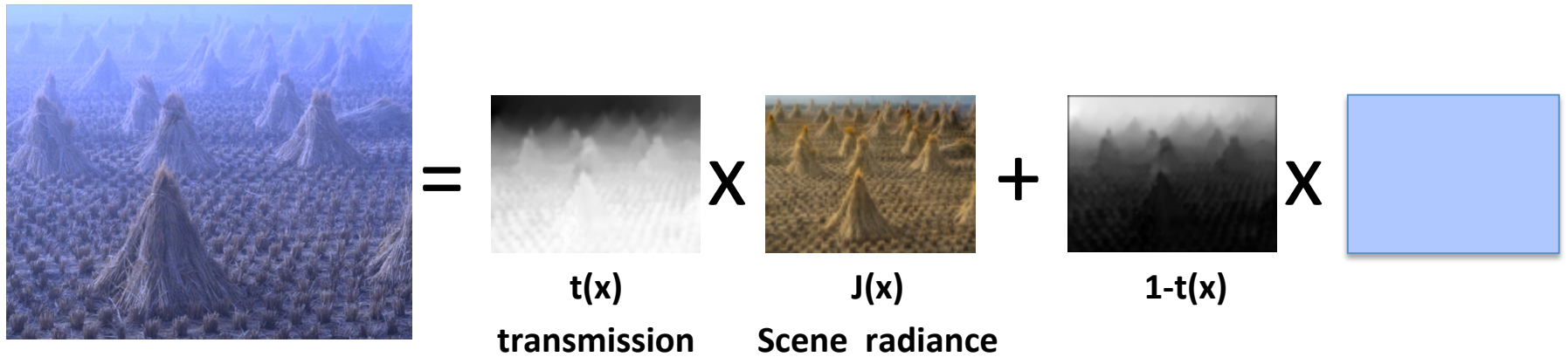
Estimate A and $t(x)$ from $I(x)$,
then calculate $J(x)$

Estimate the fog density for each pixel, and then
remove it. (light in near, and heavy in far)

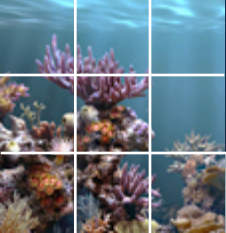
The procedure of defogging is as follows.



Dark Channel based Image Dehazing



$$\mathbf{I}(\mathbf{x}) = \mathbf{J}(\mathbf{x})t(\mathbf{x}) + \mathbf{A}(1 - t(\mathbf{x}))$$



Most local patches in haze-free outdoor images contain some pixels which have very low intensities in at least one color channel, so that for these pixels:



$$I(x) = \cancel{L_{object} t(z)} + A \cdot (1 - t(z)) \quad \text{where} \quad t = e^{-\beta z}$$

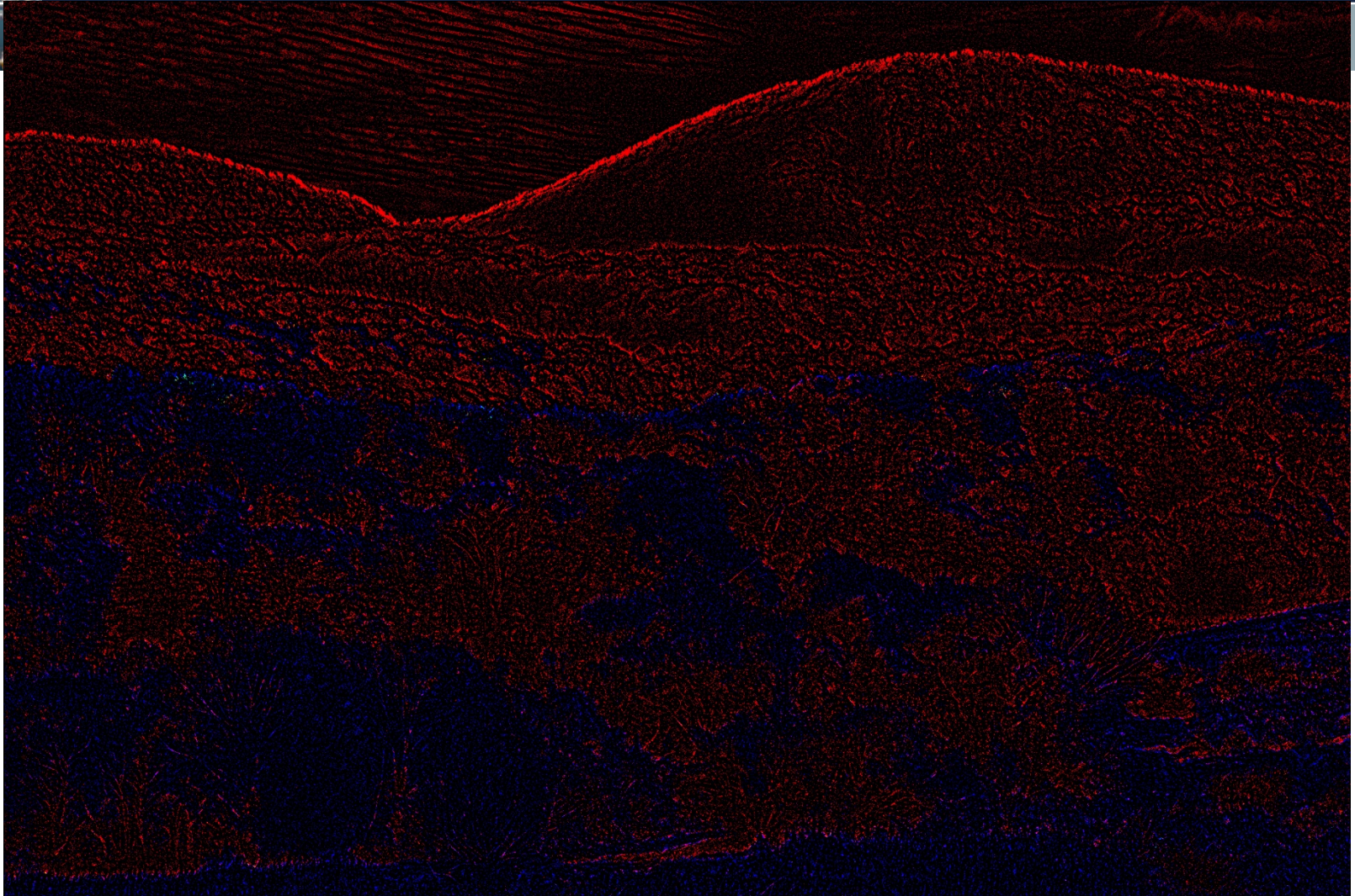
Dark channel can be defined as:

$$I^{dark}(x) = \min_{c \in \{R, G, B\}} \left(\min_{y \in \omega(x)} I^{(c)}(y) \right)$$

From here we can get transmission map t , given that we know A



Sparse 'dark channel'-based depth map



Contribution from different channels

Inpainted depth map (joint bilateral filter)



Single image dehazing



Single image dehazing

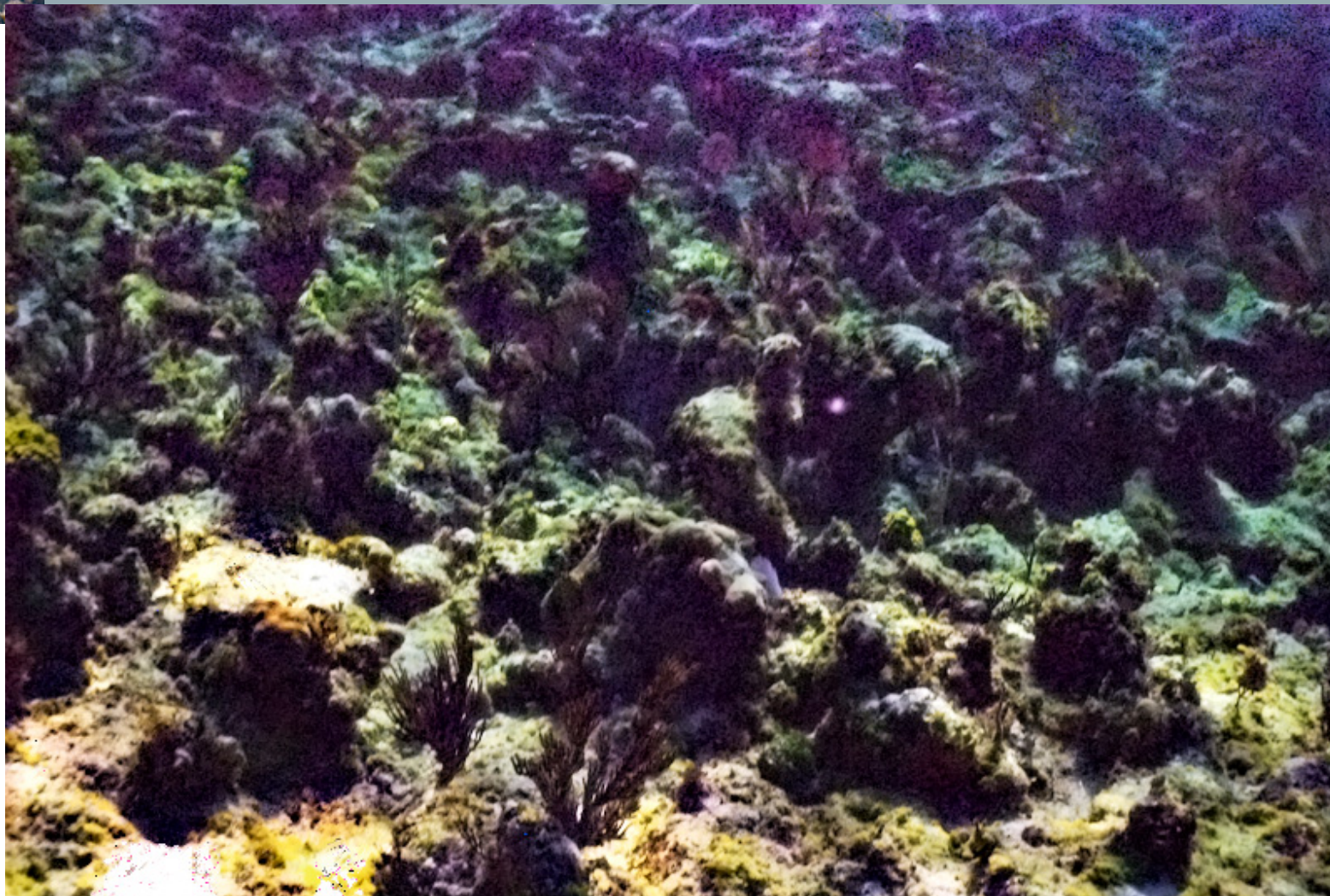


Single image dehazing



Original image

Single image dehazing



Corrected image

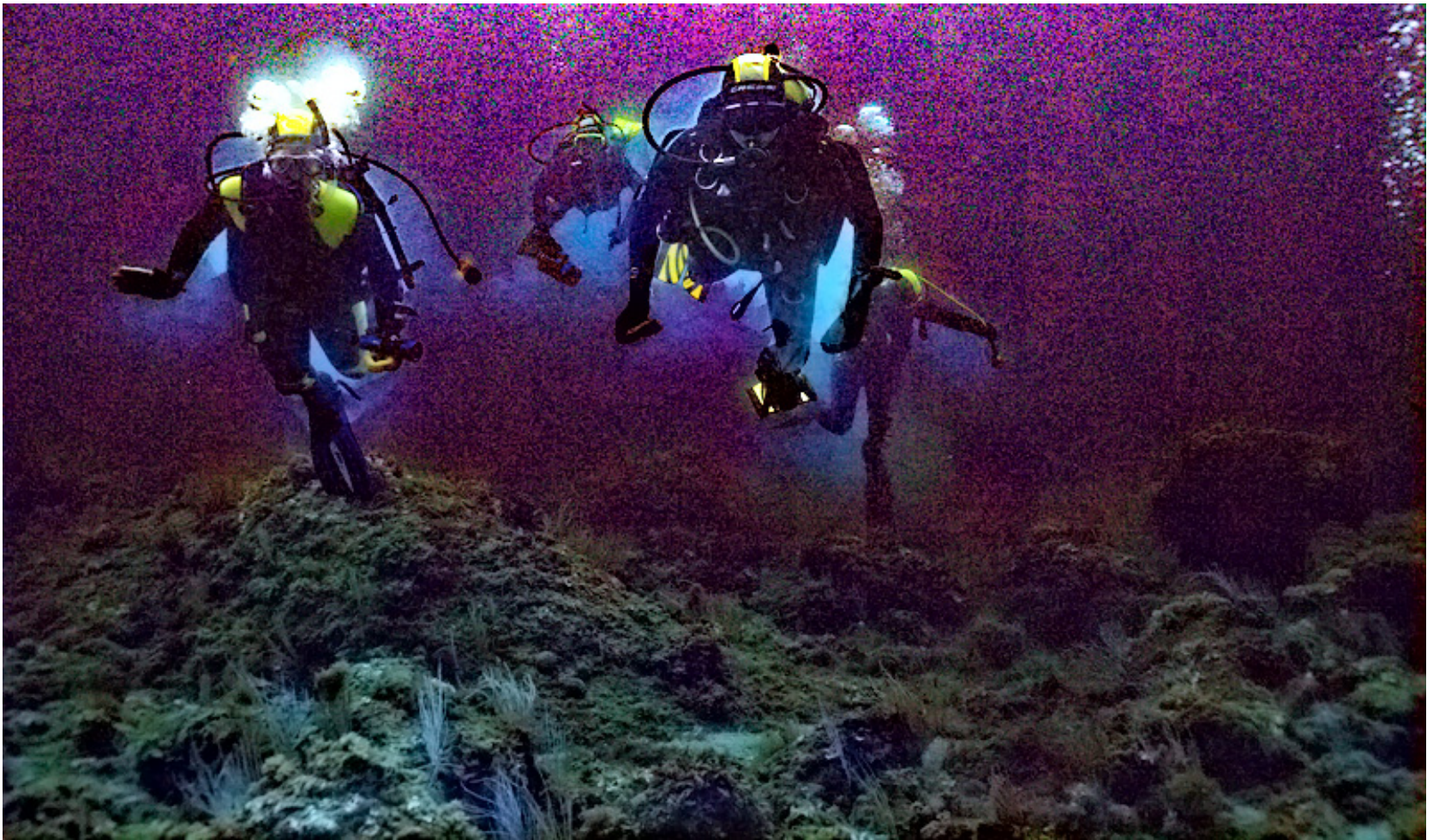
Single image dehazing



Original image

Single image dehazing – possible artifacts (color, halo, etc.)

All dark channel methods have problem (artifacts, speed)



***Artifacts, based on widely used dark channel method,
and starting from noisy, high ISO image***



Technique not using depth-maps

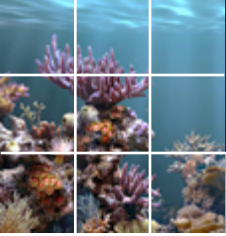
❖ A conceptually simple method

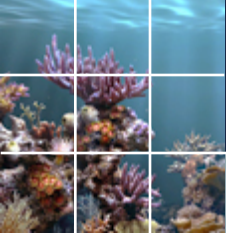
- Assumes a grey-world and uniform illumination
- Uses the Ruderman color space $L\alpha\beta$ to move the chromatic component around the white point
- Performs luminance stretching.
- Fast enough for realtime operation

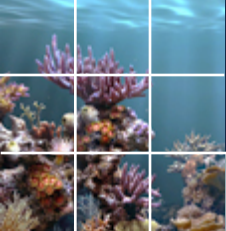
G. Bianco, M. Muzzupappa, F. Bruno, R. Garcia, L. Neumann. "A new color correction method for underwater imaging". ISPRS/CIPA Workshop on Underwater 3D Recording and Modelling, Piano di Sorrento (Napoli), Italy. 16-17 April 2015.

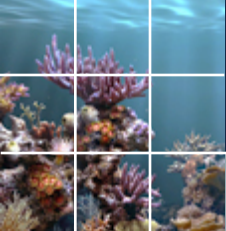
Some of our running research images

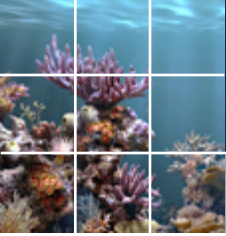




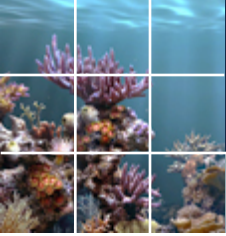


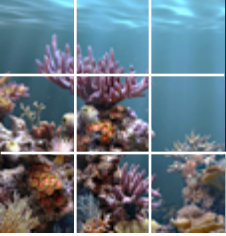


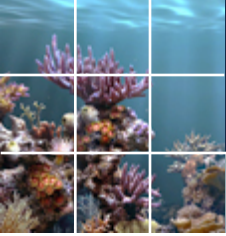




JPEG compression causes artifacts on the luminance gradient. It is better to use uncompressed images.







Camera Modeling And Calibration

Calibration Introduction – Perspective Imaging

“The Scholar of Athens,” Raphael, 1518

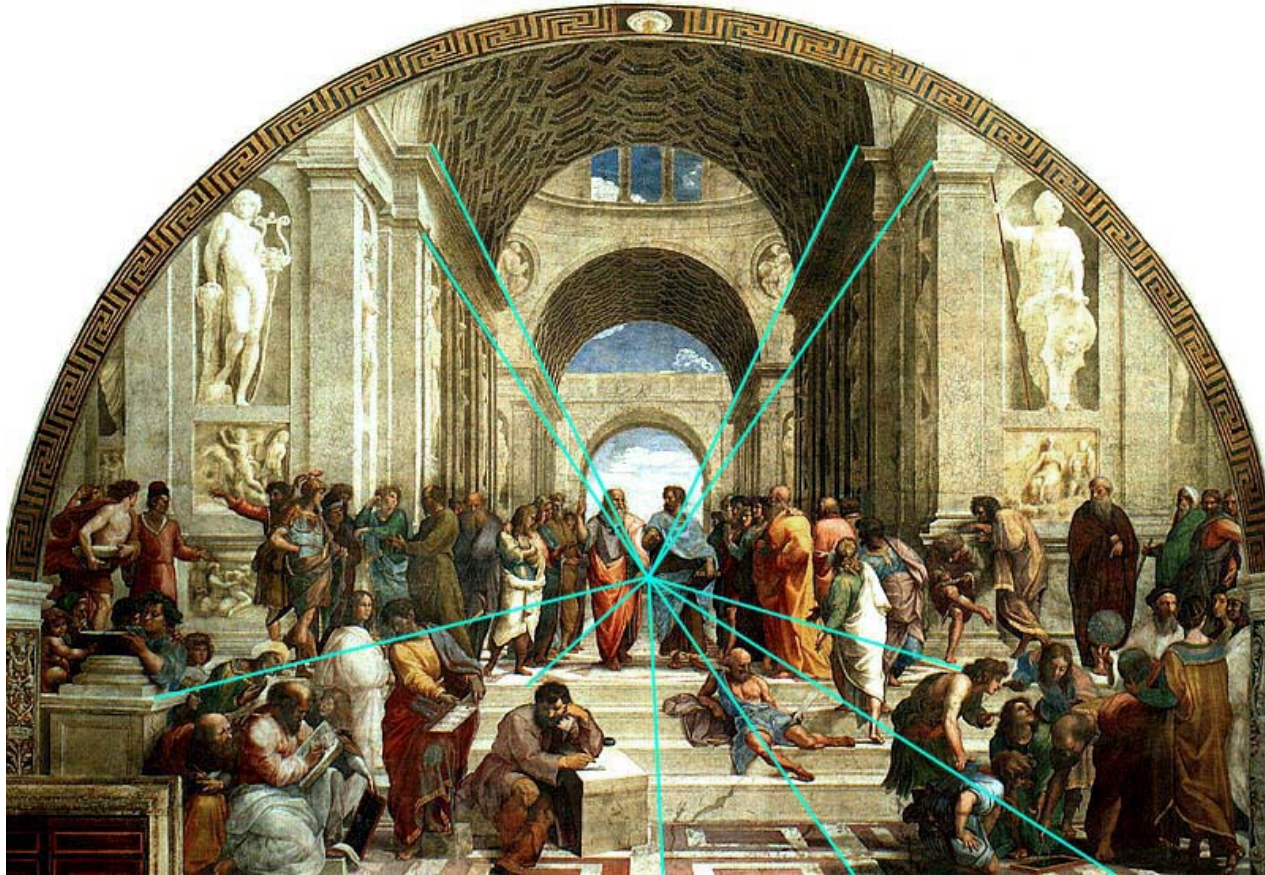
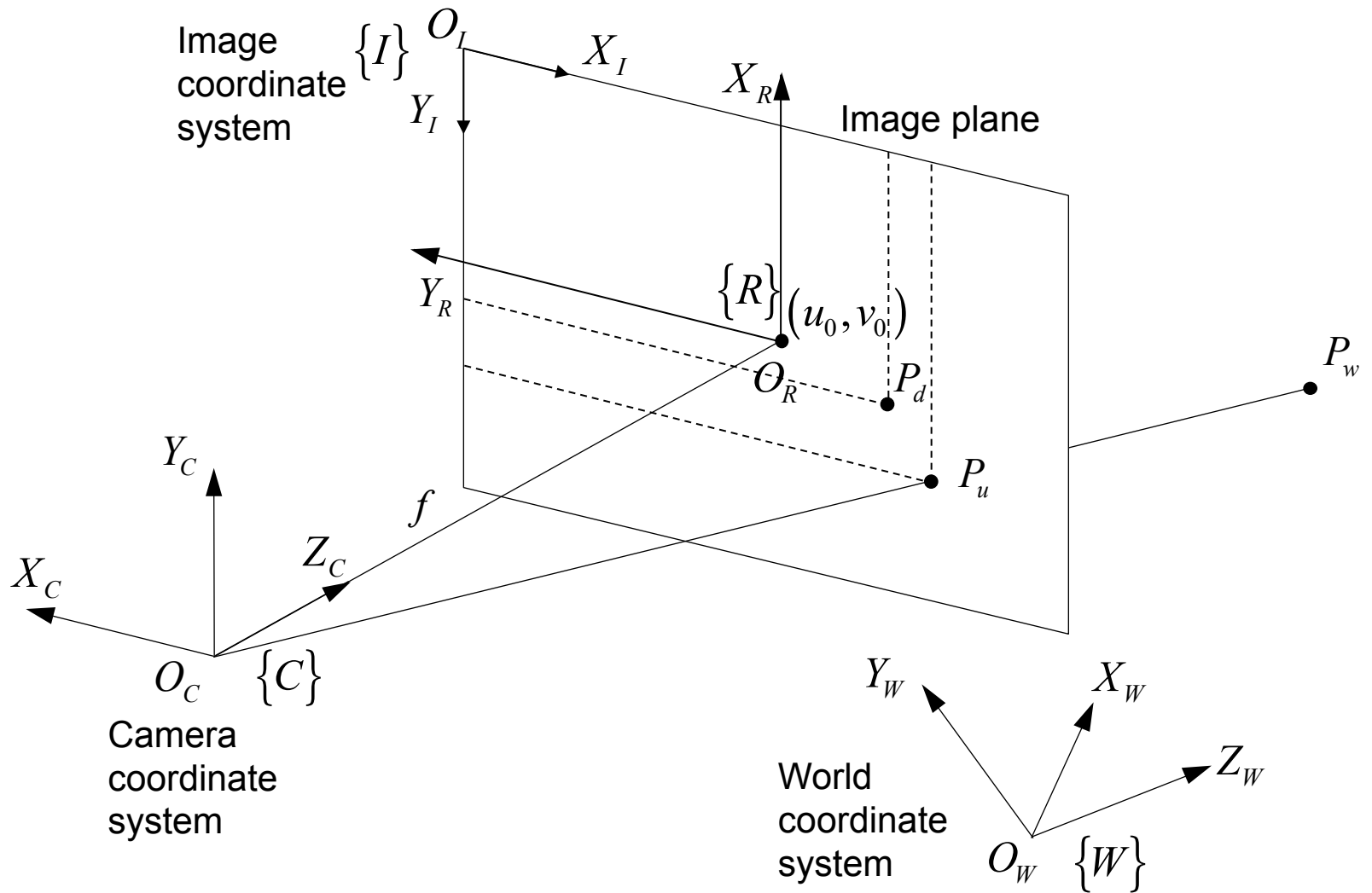
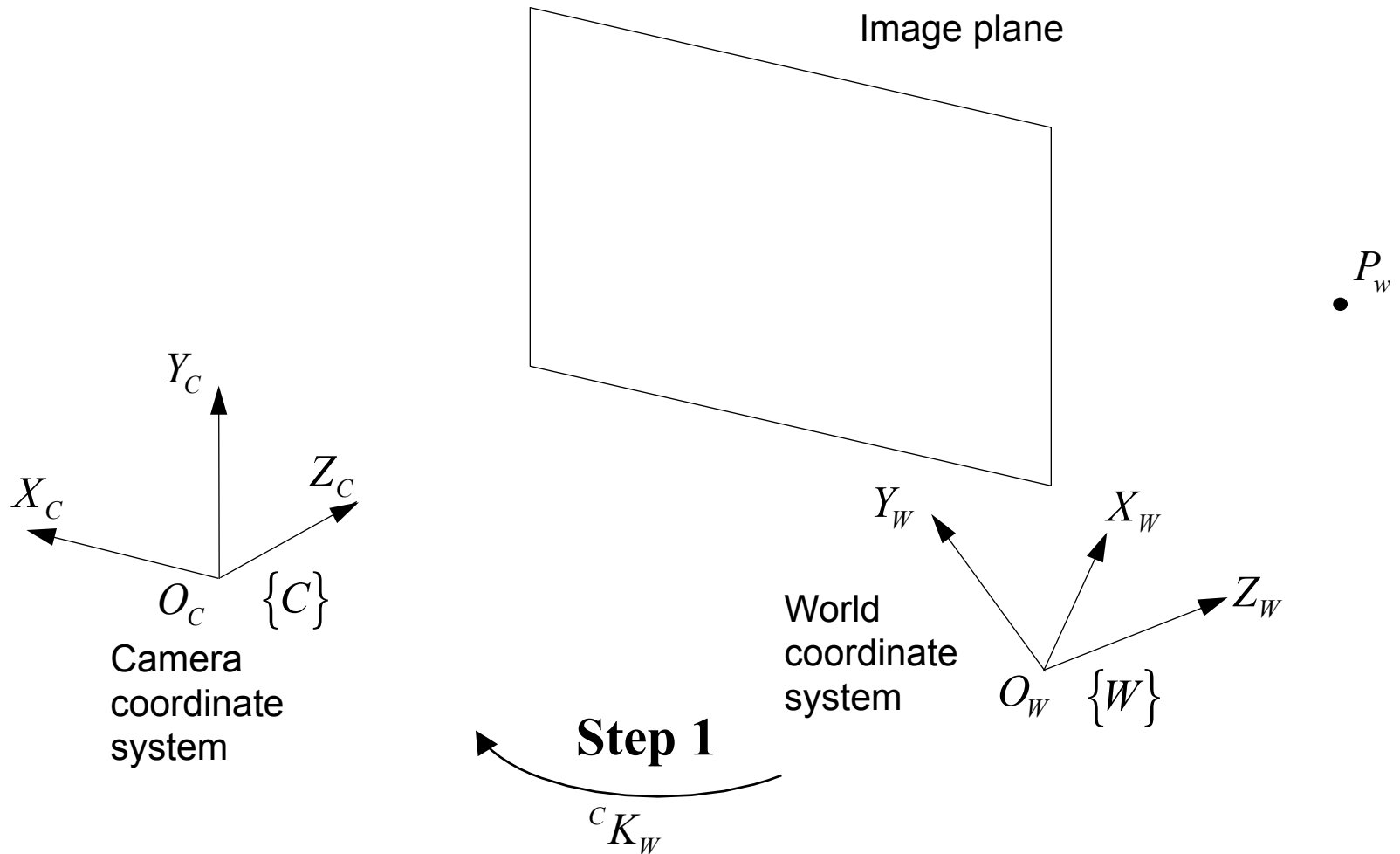


Image courtesy of C. Taylor

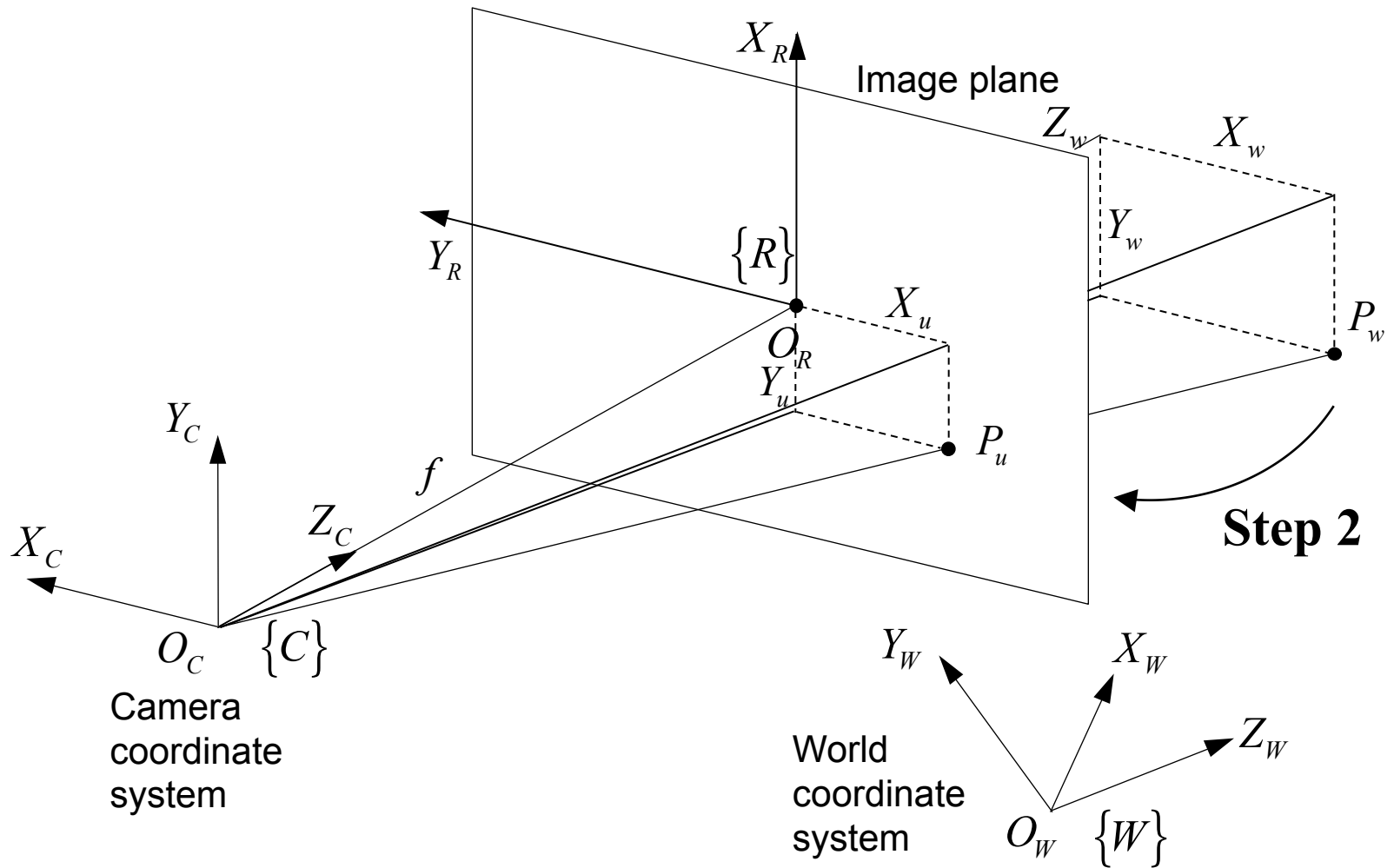
Camera Model



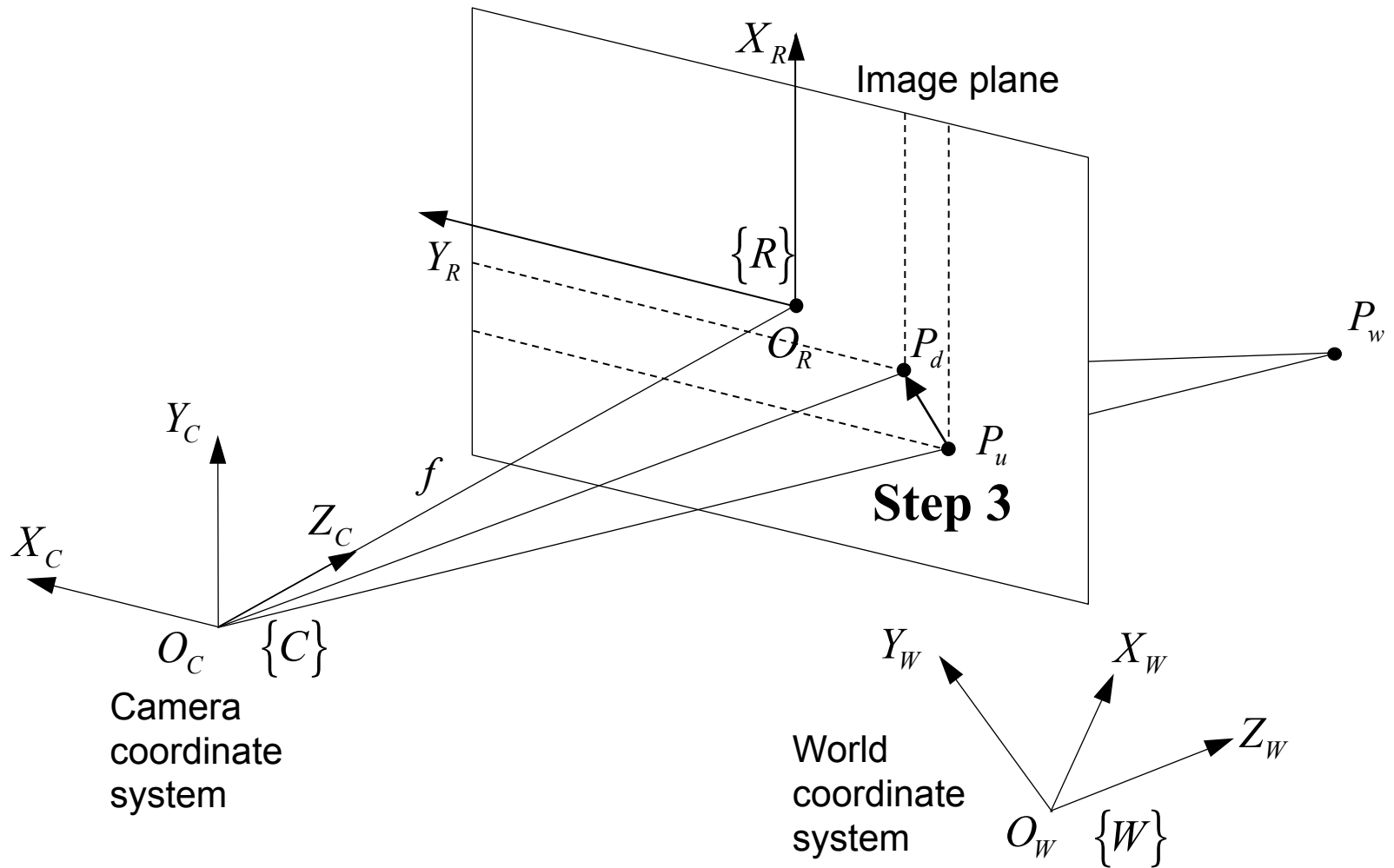
Camera Model (Step 1: World to Camera)



Camera Model (Step 2: Projection)

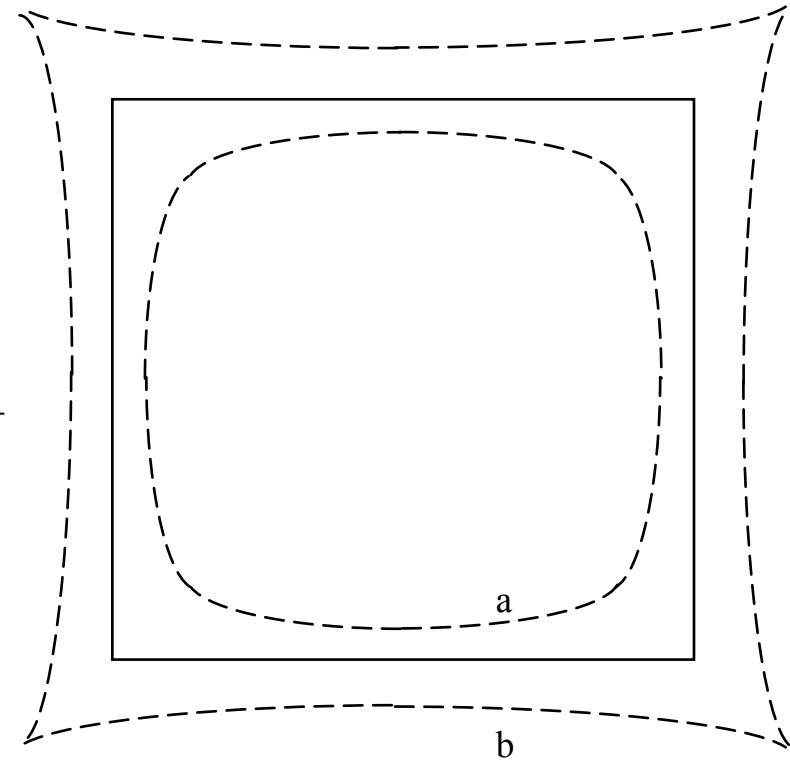
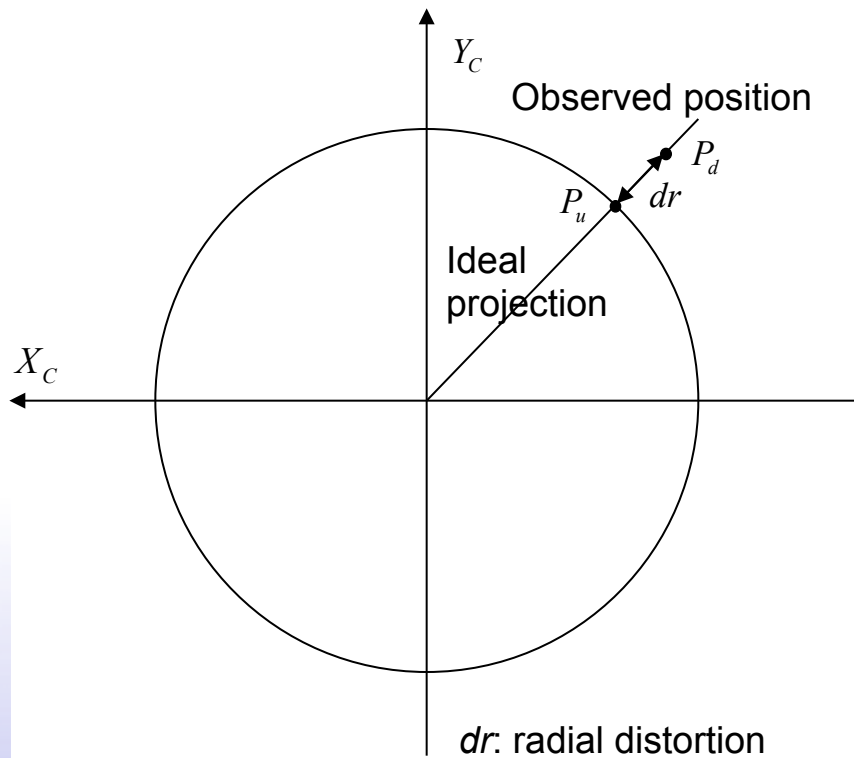


Camera Model (Step 3: Lens Distortion)



Camera Model (Step 3: Lens Distortion)

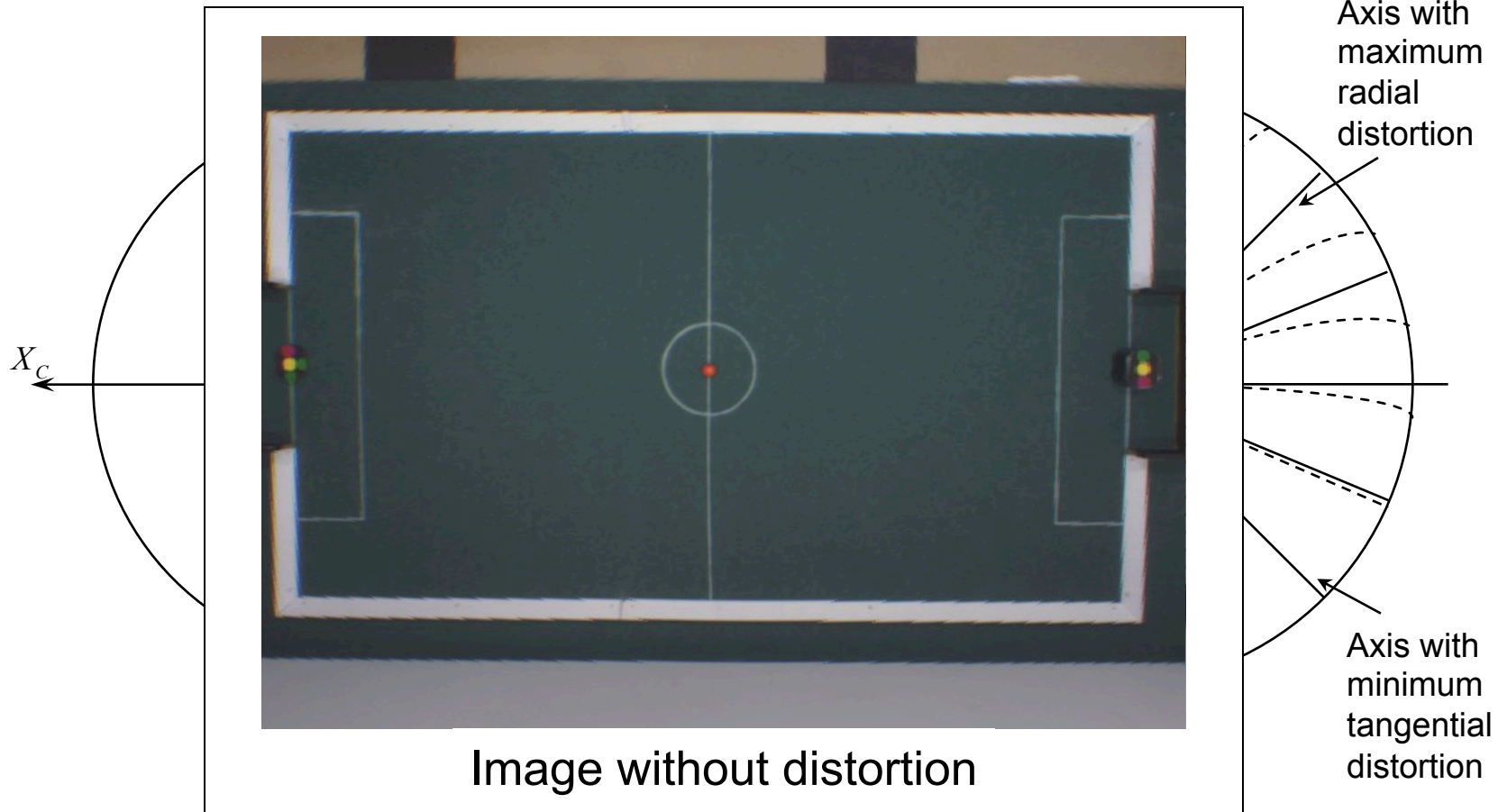
Radial Distortion



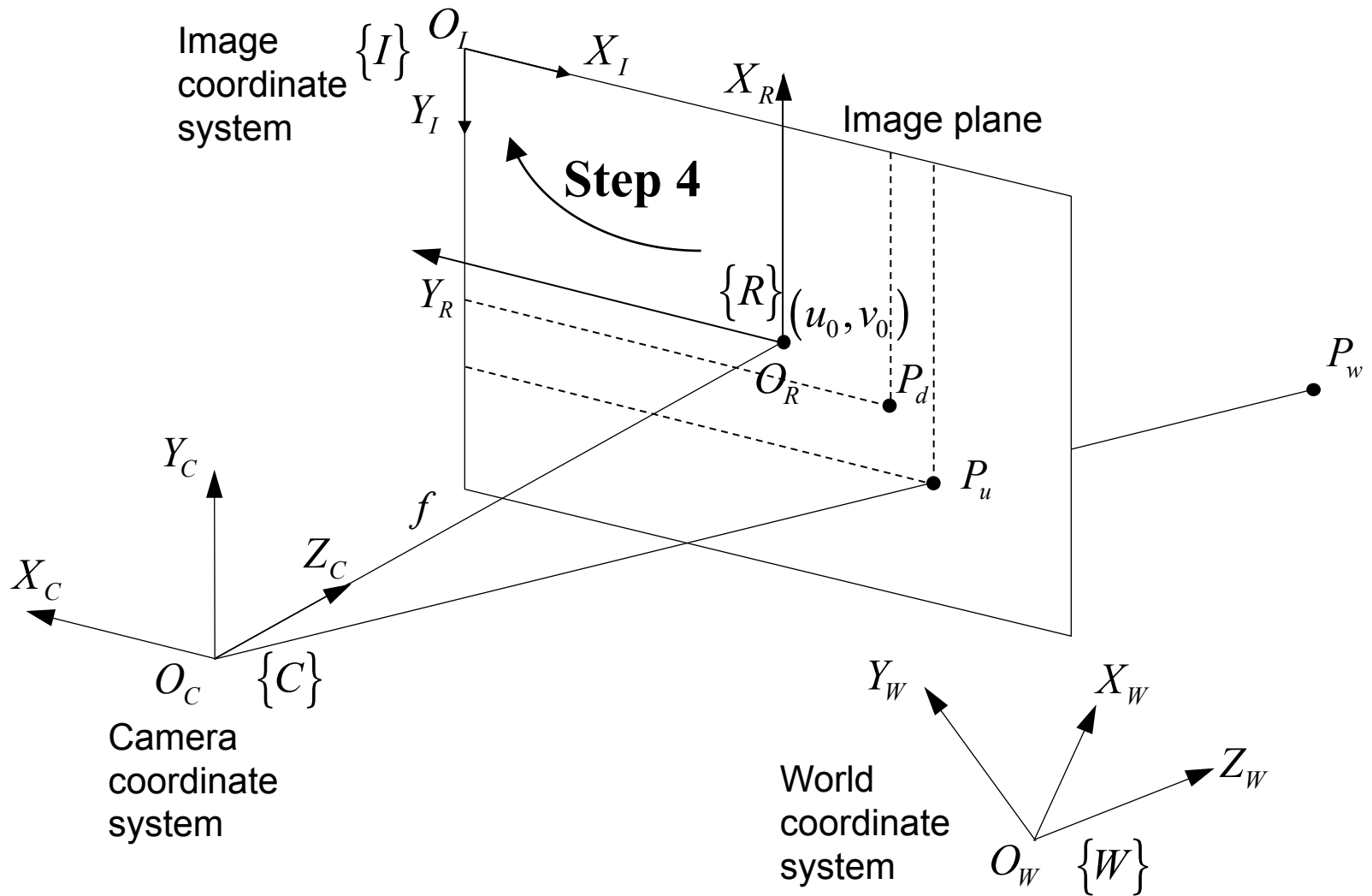
Radial distortion effect (a: negative, b: positive)

Camera Model (Step 3: Lens Distortion)

Radial and Tangential Distortion



Camera Model (Step 4: Camera to Image)



Calibration Methods

- Method of Hall
 - Linear method
 - Transformation matrix
- Method of Faugeras-Toscani
 - Linear method
 - Obtaining camera parameters
- Method of Faugeras-Toscani with distortion
 - Iterative method
 - Radial distortion

2.3.1. The Method of Hall

Assume light is captured on the image plane by a linear projection

$$\begin{pmatrix} s^I X_u \\ s^I Y_u \\ s \end{pmatrix} = \begin{pmatrix} A_{11} & A_{12} & A_{13} & A_{14} \\ A_{21} & A_{22} & A_{23} & A_{24} \\ A_{31} & A_{32} & A_{33} & A_{34} \end{pmatrix} \begin{pmatrix} {}^W X_w \\ {}^W Y_w \\ {}^W Z_w \\ 1 \end{pmatrix}$$

The matrix is defined up to a scale factor → Multiple Solutions
A component is fixed to the unity → Unique Solution

$$\begin{pmatrix} s^I X_u \\ s^I Y_u \\ s \end{pmatrix} = \begin{pmatrix} A_{11} & A_{12} & A_{13} & A_{14} \\ A_{21} & A_{22} & A_{23} & A_{24} \\ A_{31} & A_{32} & A_{33} & 1 \end{pmatrix} \begin{pmatrix} {}^W X_w \\ {}^W Y_w \\ {}^W Z_w \\ 1 \end{pmatrix}$$

2.3.1. The Method of Hall

$$\begin{pmatrix} s^I X_u \\ s^I Y_u \\ s \end{pmatrix} = \begin{pmatrix} A_{11} & A_{12} & A_{13} & A_{14} \\ A_{21} & A_{22} & A_{23} & A_{24} \\ A_{31} & A_{32} & A_{33} & 1 \end{pmatrix} \begin{pmatrix} {}^W X_w \\ {}^W Y_w \\ {}^W Z_w \\ 1 \end{pmatrix}$$

$${}^I X_u = \frac{A_{11} {}^W X_w + A_{12} {}^W Y_w + A_{13} {}^W Z_w + A_{14}}{A_{31} {}^W X_w + A_{32} {}^W Y_w + A_{33} {}^W Z_w + 1}$$

$${}^I Y_u = \frac{A_{21} {}^W X_w + A_{22} {}^W Y_w + A_{23} {}^W Z_w + A_{24}}{A_{31} {}^W X_w + A_{32} {}^W Y_w + A_{33} {}^W Z_w + 1}$$

$$A_{11} {}^W X_w - A_{31} {}^I X_u {}^W X_w + A_{12} {}^W Y_w - A_{32} {}^I X_u {}^W Y_w + A_{13} {}^W Z_w - A_{33} {}^I X_u {}^W Z_w + A_{14} = {}^I X_u$$

$$A_{21} {}^W X_w - A_{31} {}^I Y_u {}^W X_w + A_{22} {}^W Y_w - A_{32} {}^I Y_u {}^W Y_w + A_{23} {}^W Z_w - A_{33} {}^I Y_u {}^W Z_w + A_{24} = {}^I Y_u$$

2.3.1. The Method of Hall

$$A_{11} {}^W X_w - A_{31} {}^I X_u {}^W X_w + A_{12} {}^W Y_w - A_{32} {}^I X_u {}^W Y_w + A_{13} {}^W Z_w - A_{33} {}^I X_u {}^W Z_w + A_{14} = {}^I X_u$$

$$A_{21} {}^W X_w - A_{31} {}^I Y_u {}^W X_w + A_{22} {}^W Y_w - A_{32} {}^I Y_u {}^W Y_w + A_{23} {}^W Z_w - A_{33} {}^I Y_u {}^W Z_w + A_{24} = {}^I Y_u$$

$$A = \begin{pmatrix} A_{11} & A_{12} & A_{13} & A_{14} & A_{21} & A_{22} & A_{23} & A_{24} & A_{31} & A_{32} & A_{33} \end{pmatrix}^T$$

Obtaining 11 unknowns and every 2D points gives two equations

So, at least 6 points are needed. More points leads to a more accurate solution.

$$QA = B$$

$$Q_{2i-1} = \begin{pmatrix} {}^W X_{wi} & {}^W Y_{wi} & {}^W Z_{wi} & 1 & 0 & 0 & 0 & 0 & -{}^I X_{ui} {}^W X_{wi} & -{}^I X_{ui} {}^W Y_{wi} & -{}^I X_{ui} {}^W Z_{wi} \end{pmatrix}$$

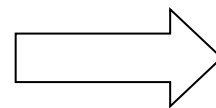
$$Q_{2i} = \begin{pmatrix} 0 & 0 & 0 & 0 & {}^W X_{wi} & {}^W Y_{wi} & {}^W Z_{wi} & 1 & -{}^I Y_{ui} {}^W X_{wi} & -{}^I Y_{ui} {}^W Y_{wi} & -{}^I Y_{ui} {}^W Z_{wi} \end{pmatrix}$$

$$B_{2i-1} = \begin{pmatrix} {}^I X_{ui} \end{pmatrix}$$

$$B_{2i} = \begin{pmatrix} {}^I Y_{ui} \end{pmatrix}$$

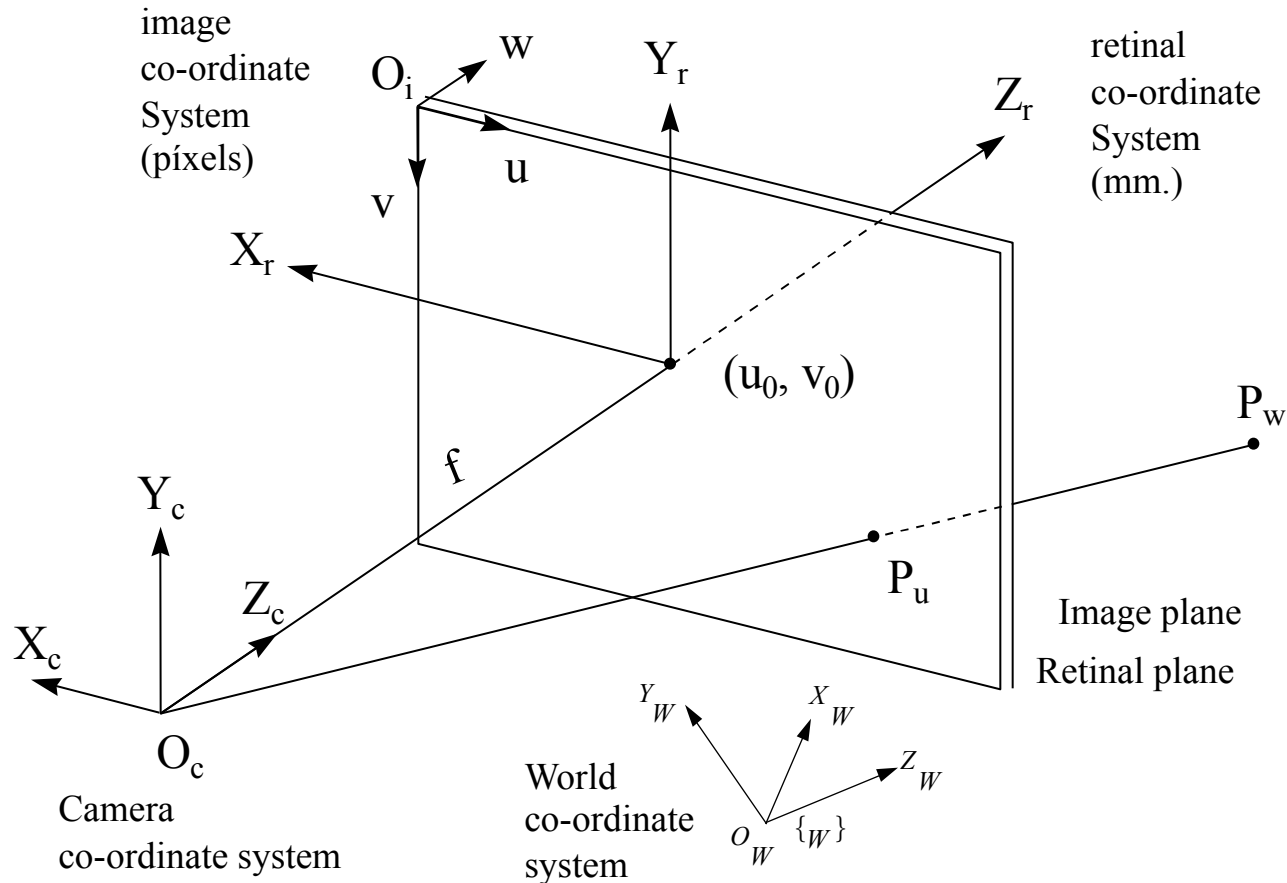
Pseudoinverse leads to a unique solution:

$$A = Q^{-1}B$$



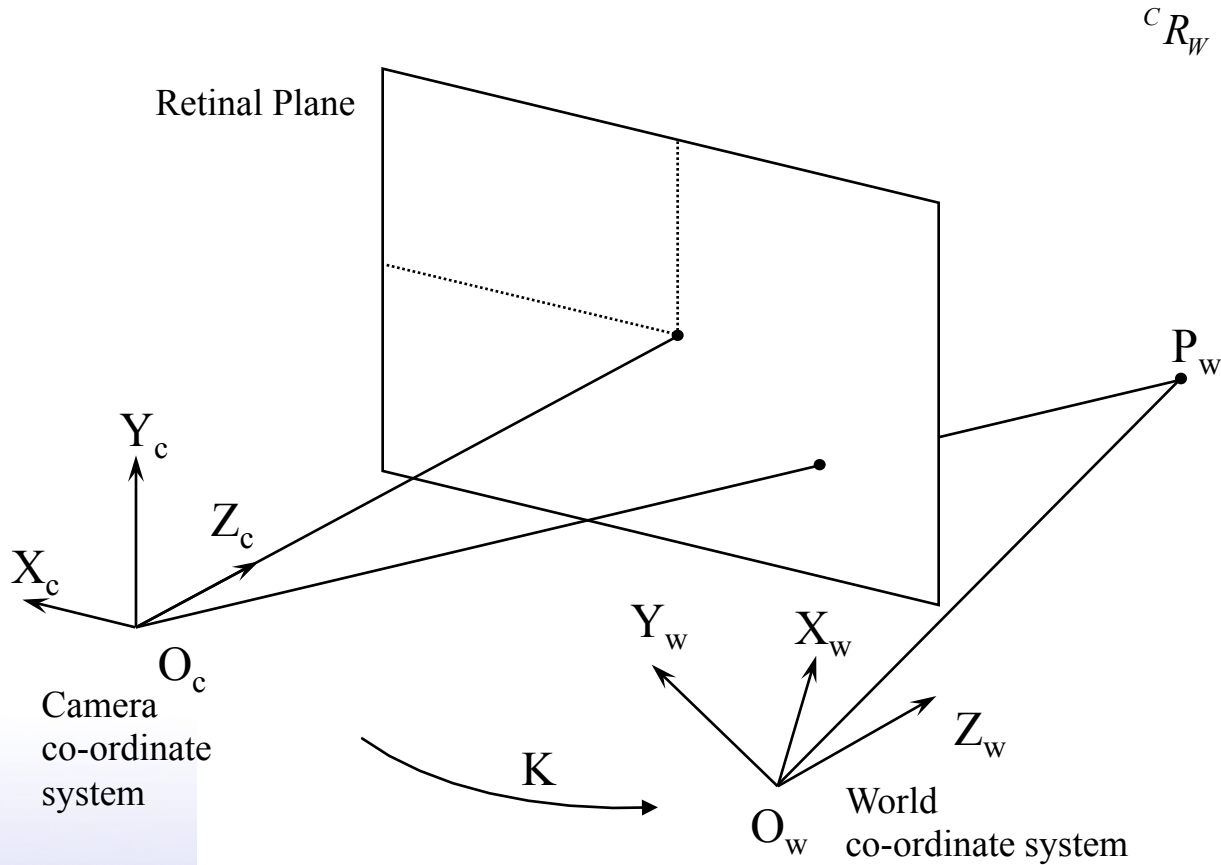
$$A = (Q^t Q)^{-1} Q^t B$$

2.3.2. The Method of Faugeras-Toscani



- **Extrinsic parameters:** Model the situation and orientation of the camera with respect to a world co-ordinate system.
- **Intrinsic parameters:** Model the behaviour of the internal geometry and the optical characteristics of the camera.

2.3.2. The Extrinsic Parameters



$${}^cR_w = Rot(X, \alpha) \cdot Rot(Y, \beta) \cdot Rot(Z, \gamma)$$

$${}^cR_w = \begin{pmatrix} r_{11} & r_{12} & r_{13} \\ r_{21} & r_{22} & r_{23} \\ r_{31} & r_{32} & r_{33} \end{pmatrix}$$

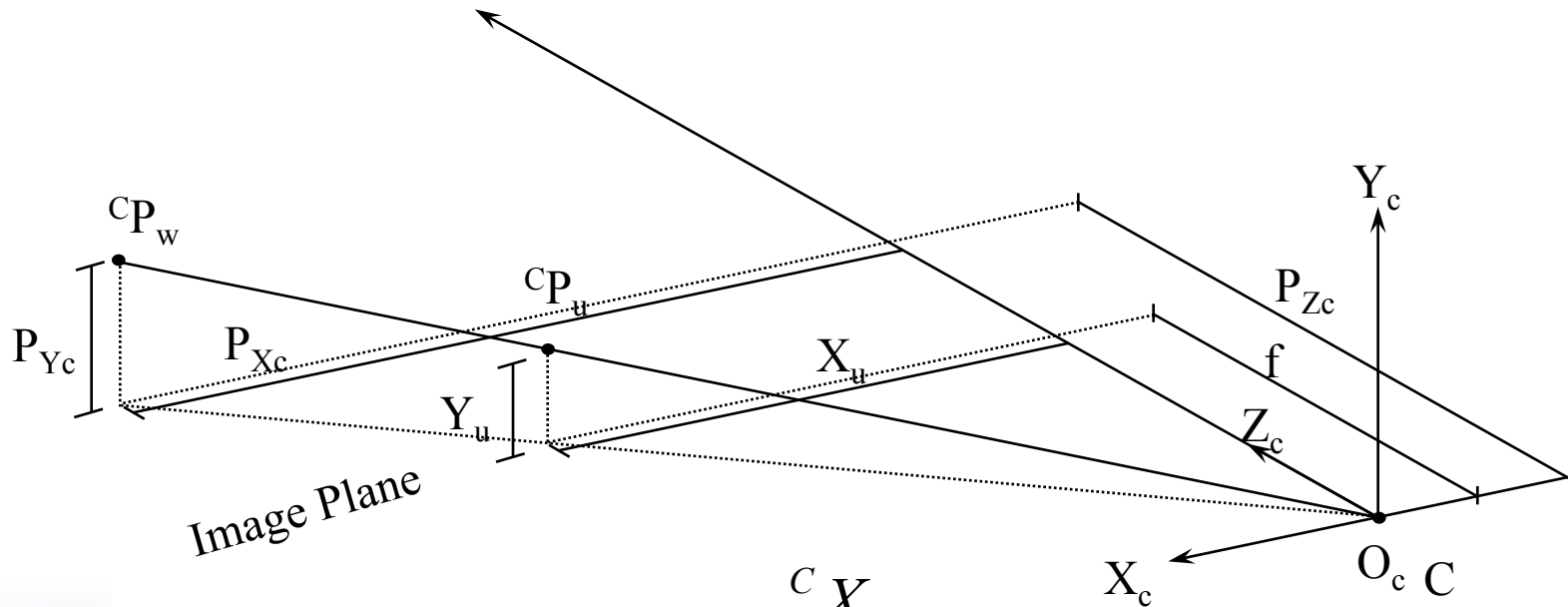
$${}^cT_w = \begin{pmatrix} t_x \\ t_y \\ t_z \end{pmatrix}$$

$$\begin{pmatrix} {}^cX_w \\ {}^cY_w \\ {}^cZ_w \end{pmatrix} = {}^cR_w \begin{pmatrix} {}^wX_w \\ {}^wY_w \\ {}^wZ_w \end{pmatrix} + {}^cT_w$$

$$\begin{pmatrix} {}^cP_w \\ 1 \end{pmatrix} = {}^cK_w \begin{pmatrix} {}^wP_w \\ 1 \end{pmatrix}$$

$${}^cK_w = \begin{pmatrix} {}^cR_{w3 \times 3} & {}^cT_{w3 \times 1} \\ \mathbf{0}_{1 \times 3} & 1 \end{pmatrix}$$

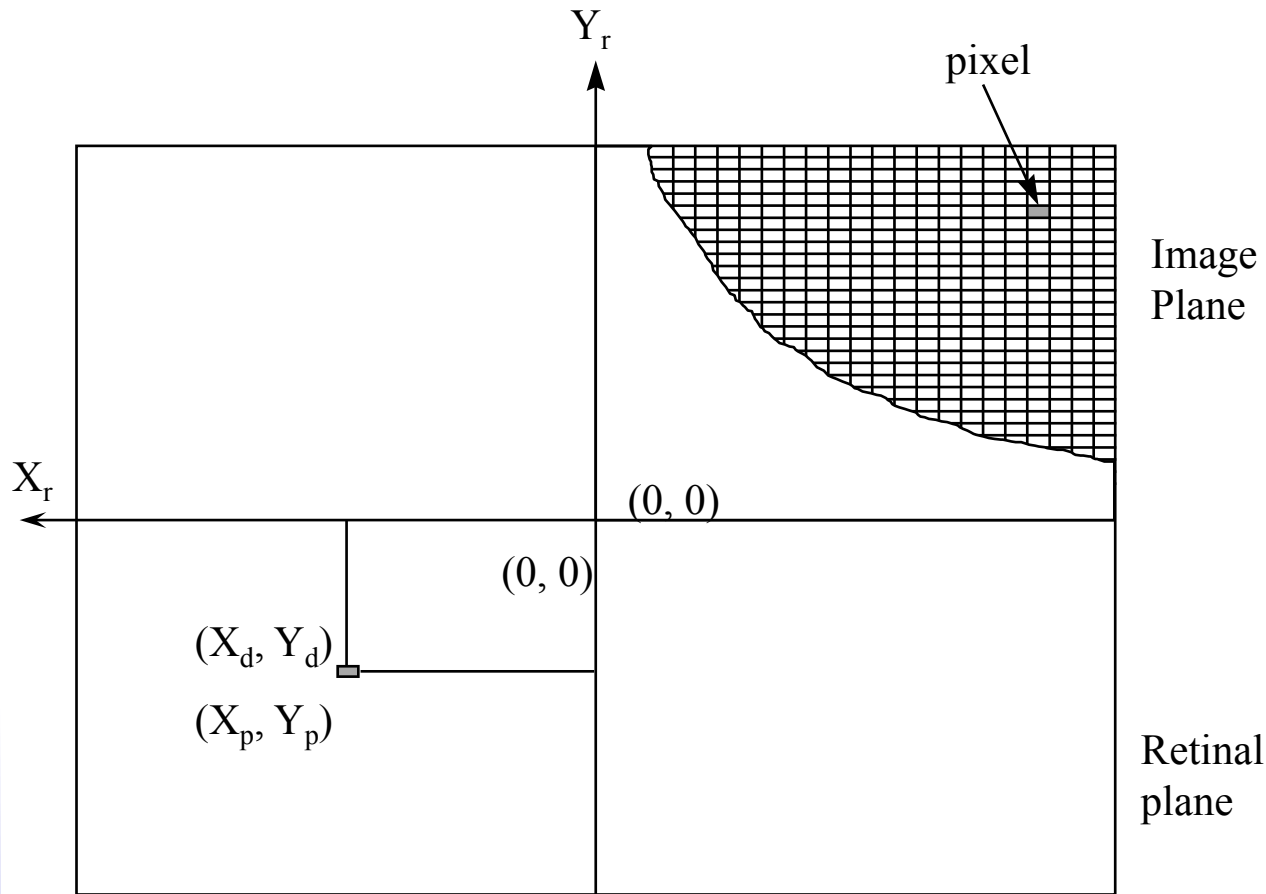
2.3.2. The Intrinsic Parameters: Ideal Projection



$${}^c X_u = f \frac{{}^c X_w}{{}^c Z_w}$$

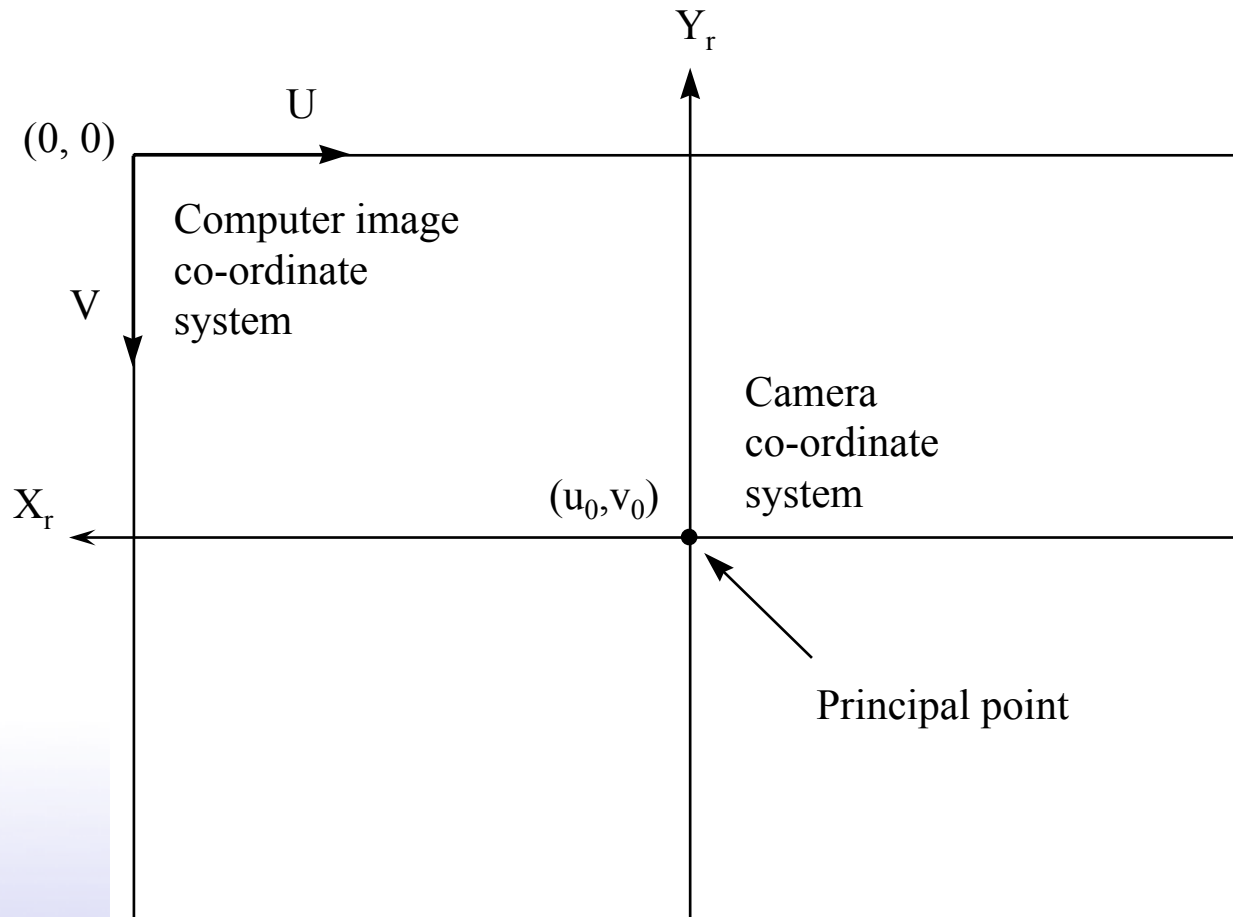
$${}^c Y_u = f \frac{{}^c Y_w}{{}^c Z_w}$$

2.3.2. The Intrinsic Parameters: Pixel Conversion



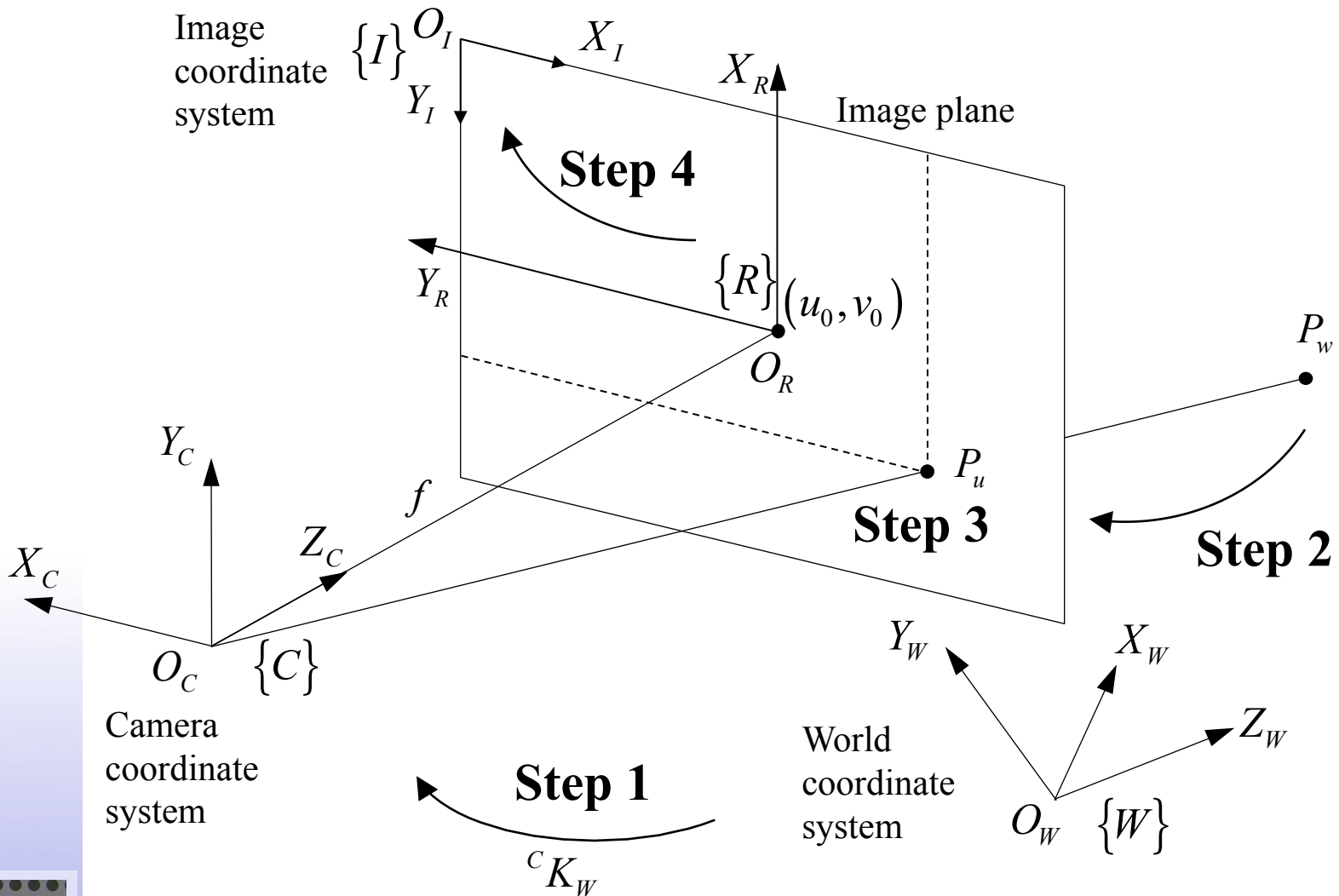
$${}^R X_d = k_u {}^C X_u$$
$${}^R Y_d = k_v {}^C Y_u$$

2.3.2. The Intrinsic Parameters: Principal Point



$${}^I X_d = -{}^R X_d + u_0$$
$${}^I Y_d = -{}^R Y_d + v_0$$

2.3.2. The Pinhole Model



2.3.2. The Pinhole Model

(X_w, Y_w, Z_w) 3D object point with respect to world co-ordinate system

Affine transformation.
Modelled parameters: \mathbf{R}, \mathbf{T}

(X_c, Y_c, Z_c) 3D object point with respect to camera co-ordinate system

Perspective transformation.
Modelled parameter: \mathbf{f}

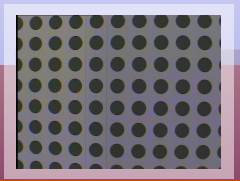
(X_u, Y_u) Ideal projection on the retinal plane

Pixel adjustment
Modelled parameters: $\mathbf{k}_u, \mathbf{k}_v$

(X_p, Y_p) Real projection on the image plane

Adaptation to the computer image buffer
Modelled parameters: $\mathbf{u}_0, \mathbf{v}_0$

(X_i, Y_i) Real projection on the image plane



2.3.2. The Pinhole Model

$$\begin{aligned}
 {}^c X_u &= f \frac{{}^c X_w}{{}^c Z_w} & {}^R X_d &= k_u {}^c X_u & {}^I X_d &= -{}^R X_d + u_0 \\
 {}^c Y_u &= f \frac{{}^c Y_w}{{}^c Z_w} & {}^R Y_d &= k_v {}^c Y_u & {}^I Y_d &= -{}^R Y_d + v_0
 \end{aligned}$$

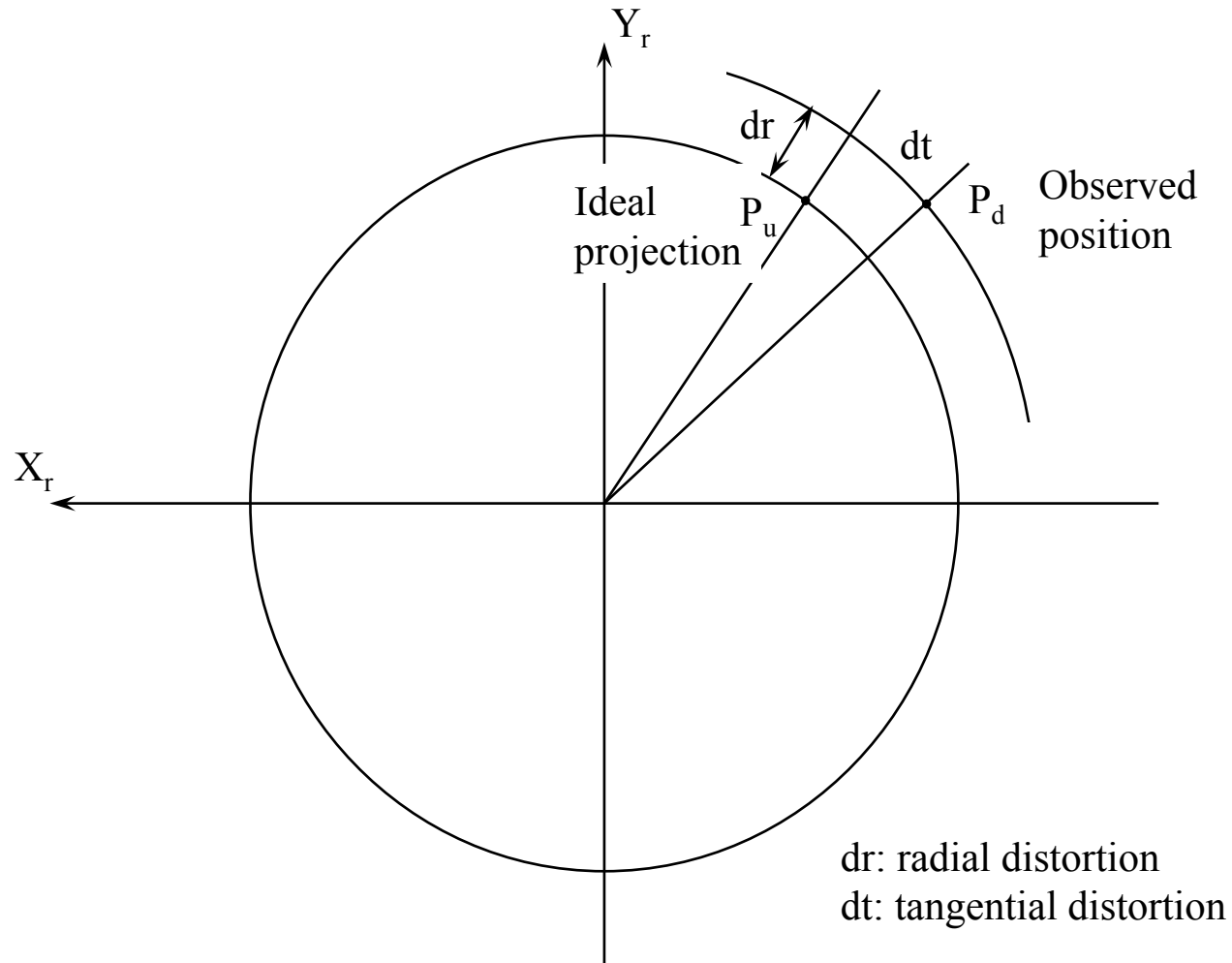
$$\begin{aligned}
 {}^I X_u &= -k_u f \frac{{}^c X_w}{{}^c Z_w} + u_0 \\
 {}^I Y_u &= -k_v f \frac{{}^c Y_w}{{}^c Z_w} + v_0
 \end{aligned}
 \quad
 \begin{pmatrix} s {}^I X_u \\ s {}^I Y_u \\ s \end{pmatrix}
 =
 \begin{pmatrix} \alpha_u & 0 & u_0 & 0 \\ 0 & \alpha_v & v_0 & 0 \\ 0 & 0 & 1 & 0 \end{pmatrix}
 \begin{pmatrix} {}^c X_w \\ {}^c Y_w \\ {}^c Z_w \\ 1 \end{pmatrix}$$

$$\begin{aligned}
 \alpha_u &= -fk_u \\
 \alpha_v &= -fk_v
 \end{aligned}$$

2.3.2. The Pinhole Model

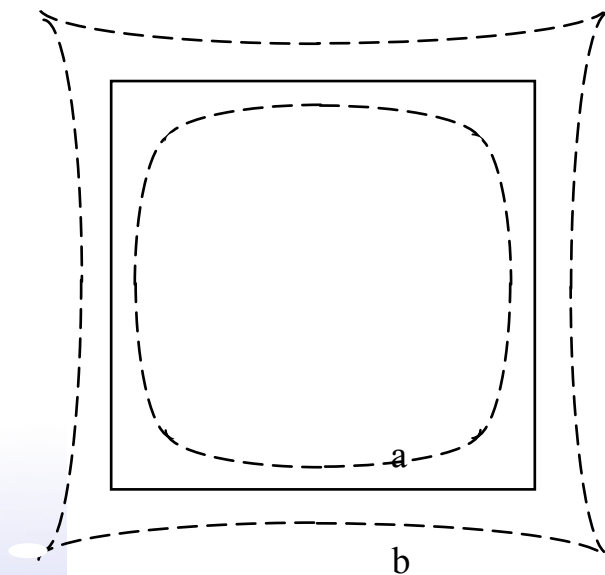
$$\begin{array}{c}
 \begin{array}{cc}
 \text{Intrínsecs} & \text{Extrínsecs}
 \end{array} \\
 \begin{pmatrix} s^I X_u \\ s^I Y_u \\ s \end{pmatrix} = \begin{pmatrix} \alpha_u & 0 & u_0 & 0 \\ 0 & \alpha_v & v_0 & 0 \\ 0 & 0 & 1 & 0 \end{pmatrix} \begin{pmatrix} r_{11} & r_{12} & r_{13} & t_x \\ r_{21} & r_{22} & r_{23} & t_y \\ r_{31} & r_{32} & r_{33} & t_z \\ 0 & 0 & 0 & 1 \end{pmatrix} \begin{pmatrix} {}^W X_w \\ {}^W Y_w \\ {}^W Z_w \\ 1 \end{pmatrix} \\
 \underbrace{\hspace{15em}} \\
 A = \begin{pmatrix} \alpha_u r_1 + u_0 r_3 & \alpha_u t_x + u_0 t_z \\ \alpha_v r_2 + v_0 r_3 & \alpha_v t_y + v_0 t_z \\ r_3 & t_z \end{pmatrix}
 \end{array}$$

Calibrating the Pinhole Model: The Extrinsics

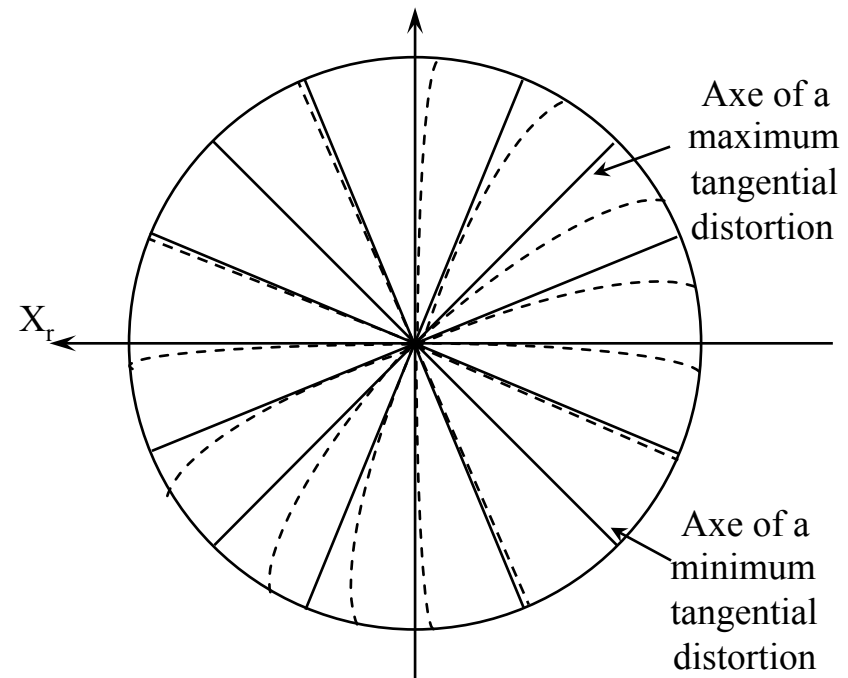


The Method of Faugeras-Toscani with distorsion

Radial distorsion effect



Tangential distorsion effect



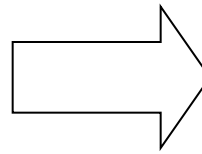
Radial distorsion is the most important and usually the only considered in calibration.

2.3.2. The Method of Faugeras-Toscani with distortion

$$D_x = {}^c X_d (k_1 r^2 + k_2 r^4 + L)$$

$$D_y = {}^c Y_d (k_1 r^2 + k_2 r^4 + L)$$

$$r = \sqrt{{}^c X_d^2 + {}^c Y_d^2}$$



k_1 is the most important component and usually sufficient in most applications.

$$\frac{X_u}{f} = \frac{P_{Xc}}{P_{Zc}}$$

$$\frac{Y_u}{f} = \frac{P_{Yc}}{P_{Zc}}$$

$$X_u = X_d + D_x$$

$$Y_u = Y_d + D_y$$

$$D_x = X_d k_1 r^2$$

$$D_y = Y_d k_1 r^2$$

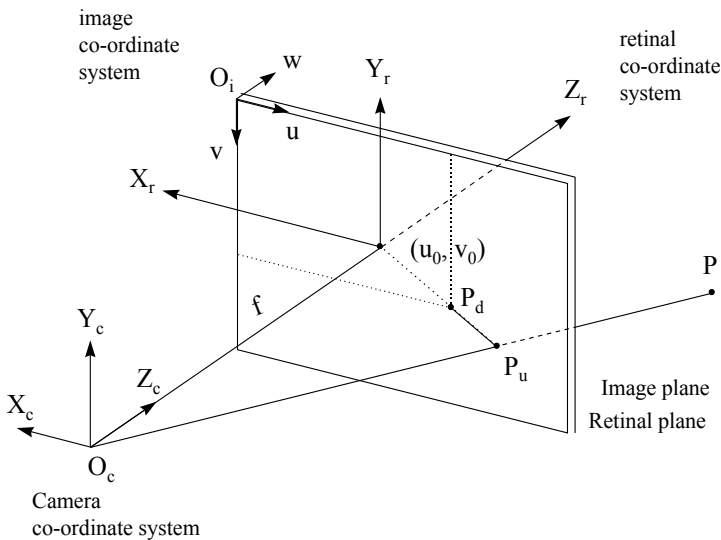
$$r = \sqrt{X_d^2 + Y_d^2}$$

$$X_p = k_u X_d$$

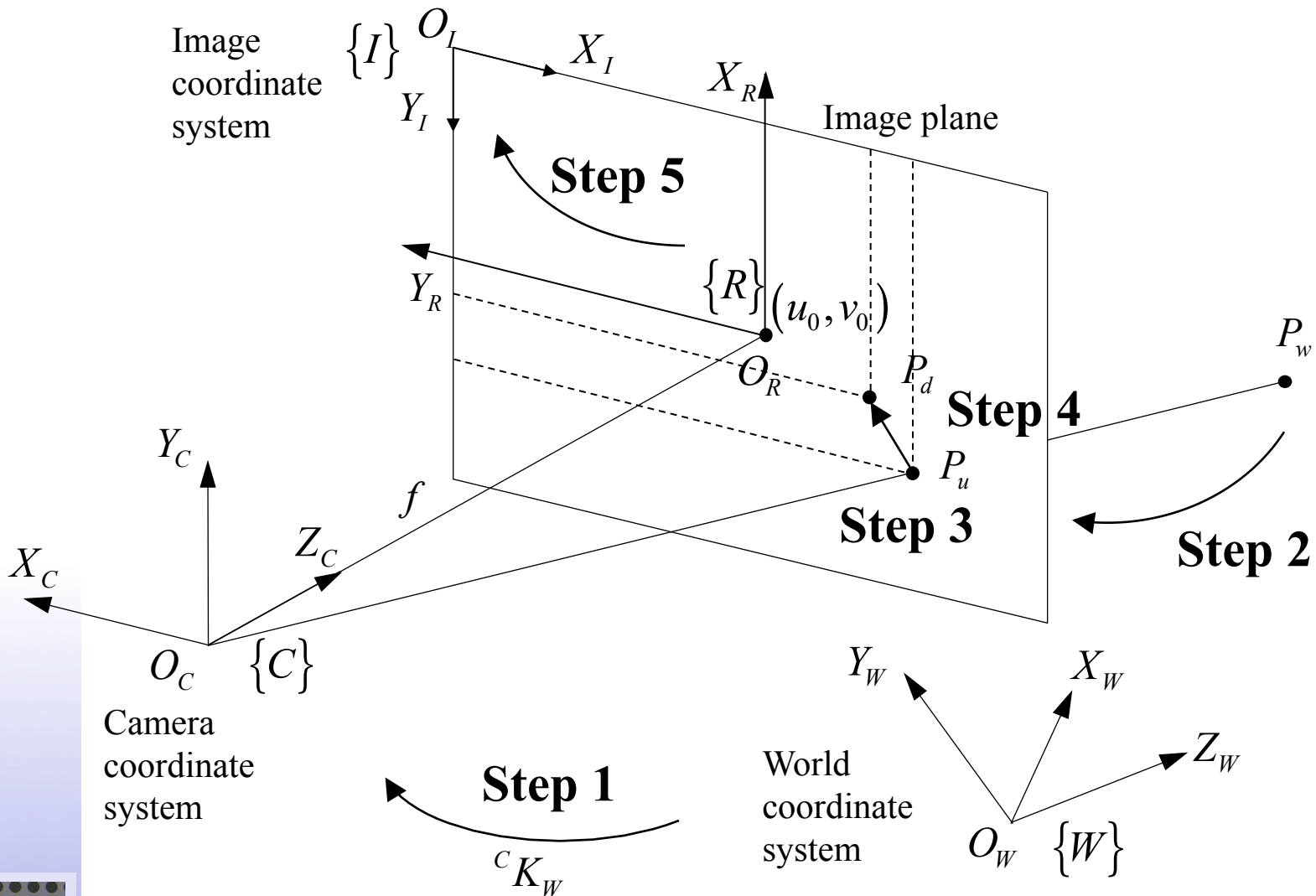
$$Y_p = k_v Y_d$$

$$X_i = -X_p + u_0$$

$$Y_i = -Y_p + v_0$$



The Method of Faugeras-Toscani with distortion



The Method of Faugeras-Toscani with distortion

(X_w, Y_w, Z_w) 3D object point with respect to world co-ordinate system

Affine transformation.
Modelled parameters: \mathbf{R}, \mathbf{T}

(X_c, Y_c, Z_c) 3D object point with respect to camera co-ordinate system

Perspective transformation.
Modelled parameter: \mathbf{f}

(X_u, Y_u) Ideal projection on the retinal plane

Radial lens distortion.
Modelled parameter: \mathbf{k}_1

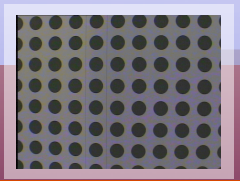
(X_d, Y_d) Real projection on the retinal plane

Pixel adjustment
Modelled parameters: $\mathbf{k}_u, \mathbf{k}_v$

(X_p, Y_p) Real projection on the image plane

Adaptation to the computer image buffer
Modelled parameters: $\mathbf{u}_0, \mathbf{v}_0$

(X_i, Y_i) Real projection on the image plane



The Method of Faugeras-Toscani with distortion

$$f \frac{{}^c X_w}{{}^c Z_w} = {}^c X_d + k_1 r^2 {}^c X_d$$

$$f \frac{{}^c Y_w}{{}^c Z_w} = {}^c Y_d + k_1 r^2 {}^c Y_d$$

$${}^c X_d = \frac{({}^I X_d - u_0)}{-k_u}$$

$${}^c Y_d = \frac{({}^I Y_d - v_0)}{-k_v}$$

$$r = \sqrt{{}^c X_d^2 + {}^c Y_d^2}$$

$$\begin{pmatrix} {}^c X_w \\ {}^c Y_w \\ {}^c Z_w \\ 1 \end{pmatrix} = {}^c K_w \begin{pmatrix} {}^w X_w \\ {}^w Y_w \\ {}^w Z_w \\ 1 \end{pmatrix}$$

The model is NON LINEAR 

Iterative minimisation:

- Newton-Raphson
- Levenberg-Marquardt

Underwater imaging

Pinhole camera model

Standard distortion models don't cover all cases! (Wide-angle, fisheye, etc...)

For example, GoPro Hero cameras have extreme wide-angle lenses:



Using OpenCV
standard distortion model



Underwater imaging

Fisheye Distortion Model (Kannala and Brandt, 2006)

Let $P=(x,y,z)$ be a point in 3D coordinates in the camera world frame. The pinhole projection coordinates of P are:

$$a = \frac{x}{z} \quad b = \frac{y}{z} \quad r^2 = a^2 + b^2$$
$$\theta = \text{atan}(r)$$

The distorted point coordinates are:

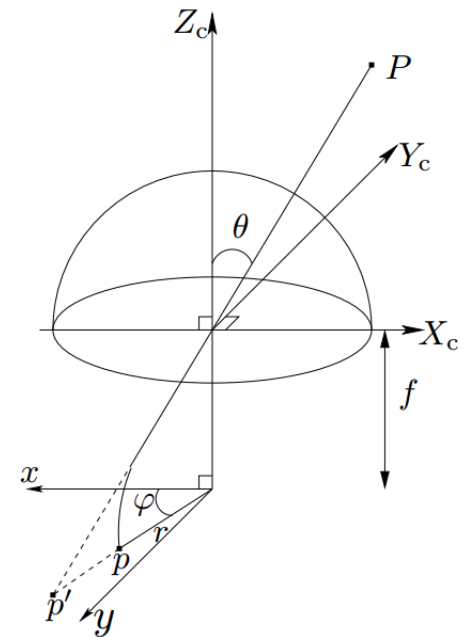
$$x' = \frac{\theta_d}{r} x \quad y' = \frac{\theta_d}{r} y$$

$$\theta_d = \theta(1 + k_1\theta^2 + k_2\theta^4 + k_3\theta^6 + k_4\theta^8)$$

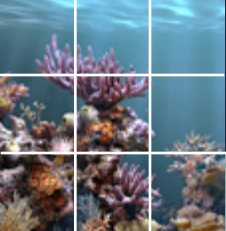
The distorted pixel coordinates are:

$$u = f_x(x' + \alpha y') + c_x$$

$$v = f_y y' + c_y$$



Underwater imaging



Underwater imaging

Omnidirectional Multicamera Systems (OMS)



OMS Calibration

1. Individual Intrinsic calibration

Physical parameters of each camera according to the model used

2. Extrinsic calibration

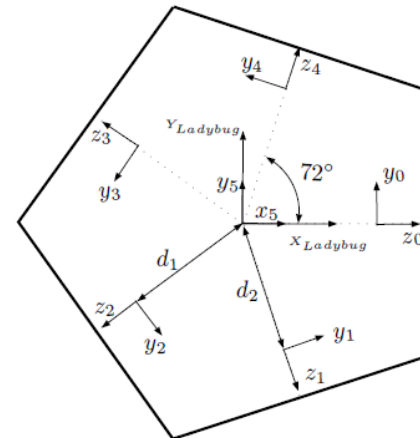
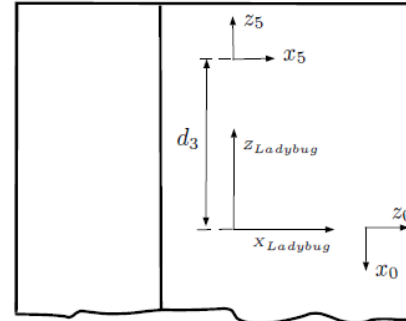
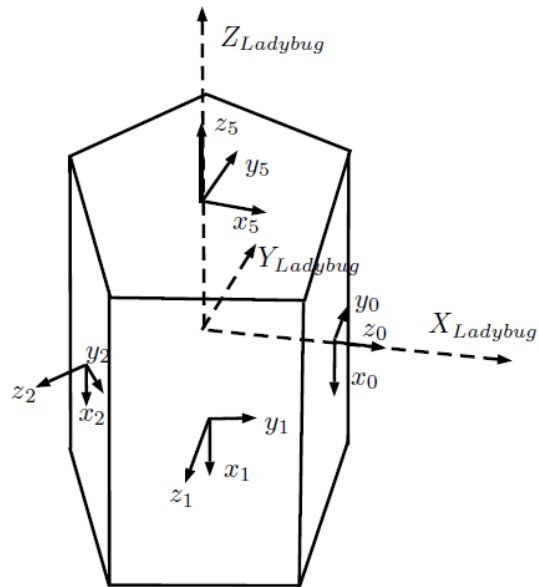
Geometric relationship between the cluster of cameras

3. Underwater calibration

Geometric relationship between the cameras and the underwater housing

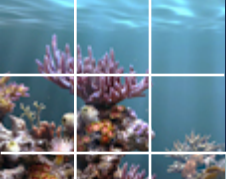
Underwater imaging

Extrinsic calibration



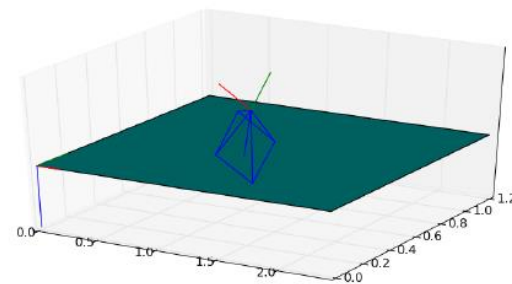
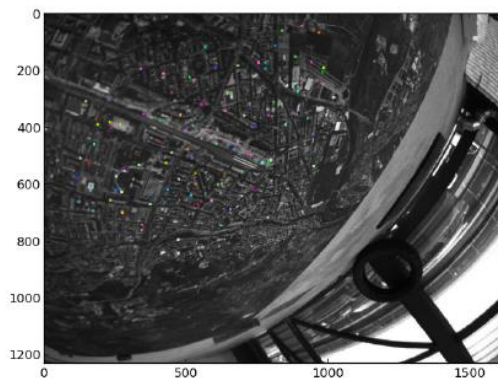
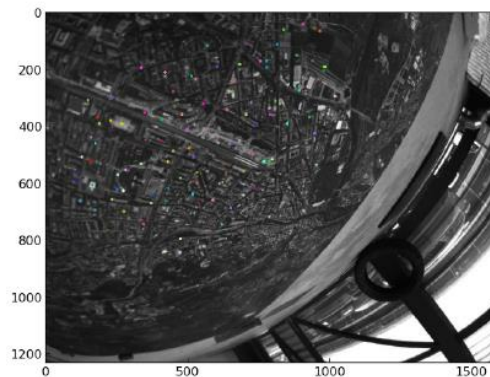
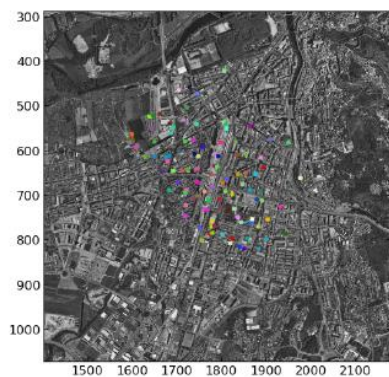
Extrinsic calibration

- Take shots of a known poster from different orientations and positions
- For every image, find matches between original poster and image
- For every frame image, solve the camera pose problem using initial values.
- Optimize parameters and pose of poster for every frame to minimize reprojection error through Levenberg-Marquardt algorithm.



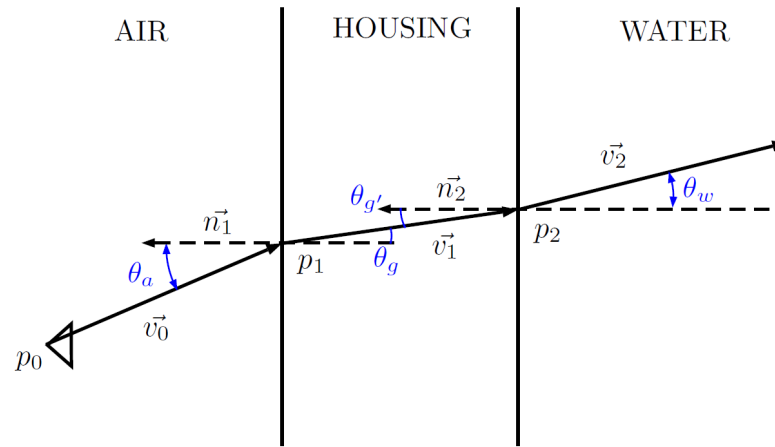
Underwater imaging

Extrinsic calibration



Underwater imaging

Underwater calibration: Ray tracing

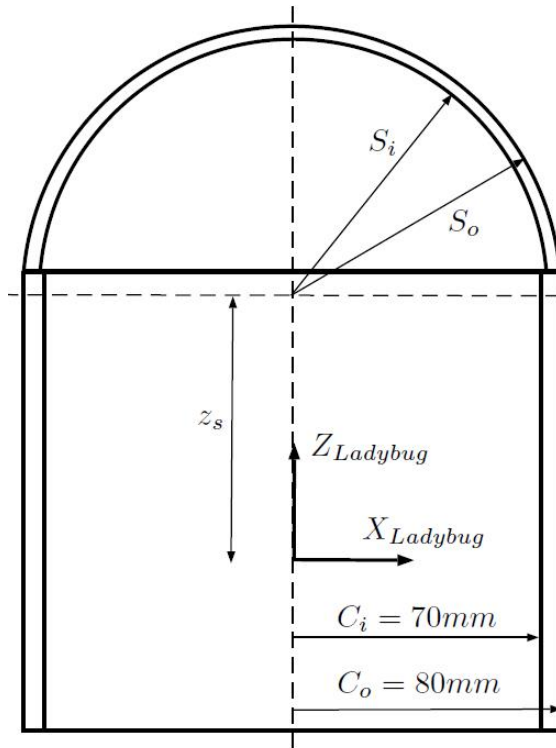


$$\sin(\theta_a) \cdot n_{air} = \sin(\theta_g) \cdot n_{PMMA}$$

$$\vec{v}_1 = -\frac{n_{air}}{n_{PMMA}} \vec{v}_0 + \left(\frac{n_{air}}{n_{PMMA}} (\vec{v}_0 \cdot \vec{n}_1) - \sqrt{1 - \left(\frac{n_{air}}{n_{PMMA}} \right)^2 \cdot (1 - (\vec{v}_0 \cdot \vec{n}_1)^2)} \right) \cdot \vec{n}_1$$

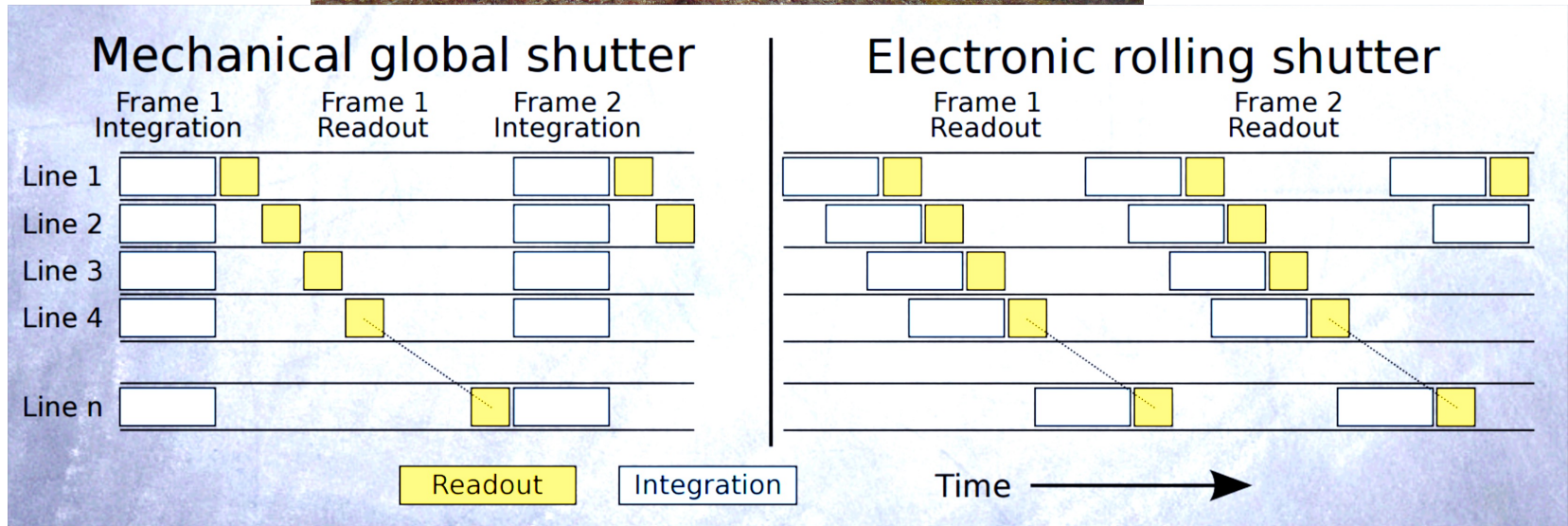
Underwater imaging

Underwater calibration



Underwater imaging

❖ Rolling Shutter





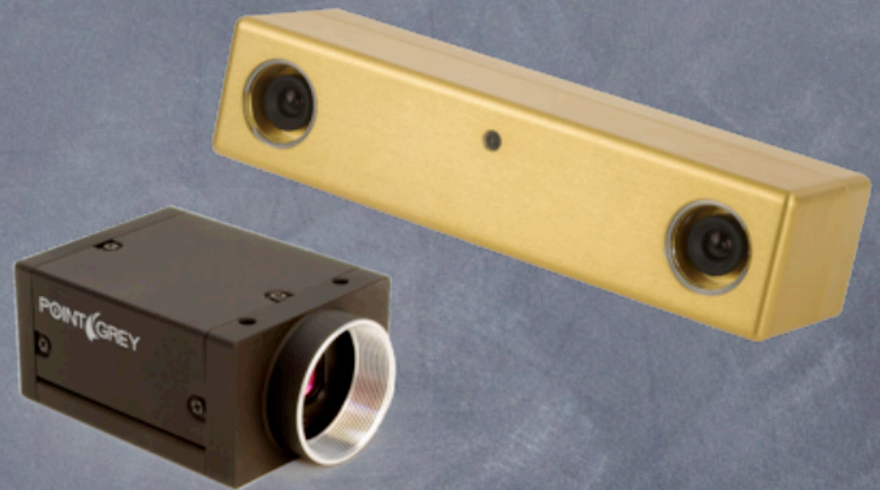
Underwater imaging

CMOS and CCD markets 2012

- CCD sensors in Astronomy and MachineVision



Spectral Instruments
12MP CCD 95x95mm



PointGrey Research
Gazelle2 and Bumblebee2
Machine Vision cameras

Underwater imaging

❖ Rolling Shutter

CMOS and CCD markets 2012

👁 CMOS sensors everywhere else



Hand-held devices
with cameras



Camcorders



compact and
SLR cameras



Robots and toys



Consumer Structured Light
Sensors (e.g. Kinect)



High-end
motion-picture cameras

Underwater imaging

❖ Rolling Shutter

It is still an open research problem



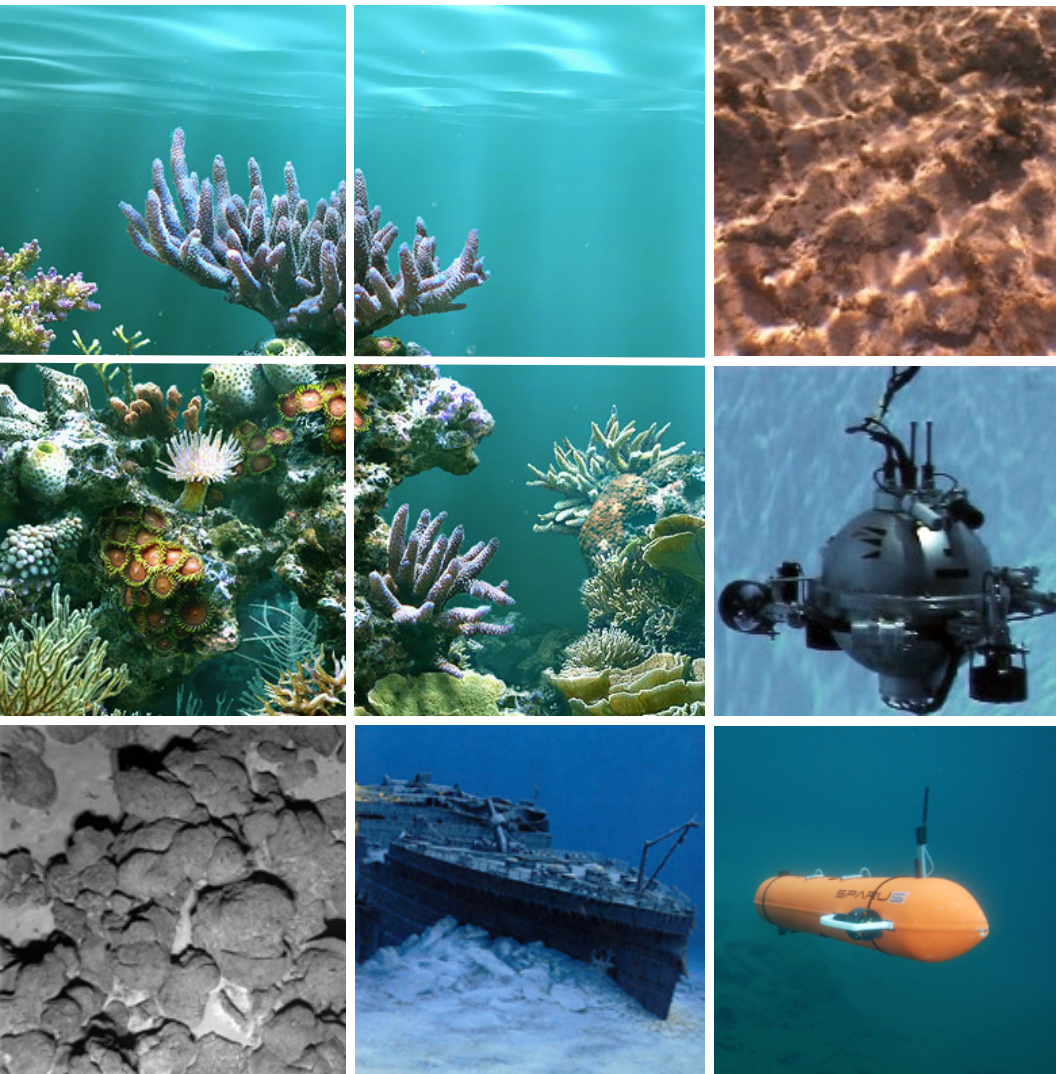
Camera Pan



Image Plane Rotation



Moving objects



Thank You !

<http://vicorob.udg.edu/>